Review Article

The closed-head impact model of engineered rotational acceleration (CHIMERA) as an application for traumatic brain injury pre-clinical research: A status report

Eileen H. McNamara[a,b,1], Antigone A. Grillakis[a,b,1], Laura B. Tucker[b,c], Joseph T. McCabe[a,b,c,*]

[a] Neuroscience Graduate Program, F.E. Hébert School of Medicine, Uniformed Services University of the Health Sciences, 4301 Jones Bridge Road, Bethesda, MD 20817-4799, USA
[b] Department of Anatomy, Physiology & Genetics, F.E. Hébert School of Medicine, Uniformed Services University of the Health Sciences, 4301 Jones Bridge Road, Bethesda, MD 20817-4799, USA
[c] Pre-Clinical Studies Core, Center for Neuroscience and Regenerative Medicine, F.E. Hébert School of Medicine, Uniformed Services University of the Health Sciences, 4301 Jones Bridge Road, Bethesda, MD 20817-4799, USA

ARTICLE INFO

ABSTRACT

Closed-head traumatic brain injury (TBI) is a worldwide concern with increasing prevalence and cost to society. Rotational acceleration is a primary mechanism in TBI that results from tissue strains that give rise to diffuse axonal injury. The Closed-Head Impact Model of Engineered Rotational Acceleration (CHIMERA) was recently introduced as a method for the study of impact acceleration effects in pre-clinical TBI research. This review provides a survey of the published literature implementing the CHIMERA device and describes pathological, imaging, neurophysiological, and behavioral findings. Findings show CHIMERA inflicts damage in white matter tracts as a key area of injury. Behaviorally, repeated studies have shown motor deficits and more chronic cognitive effects after CHIMERA injury. Good progress with model application has been accomplished by investigators attending to what is required for model validation. However, the majority of CHIMERA studies only utilize adult male mice. To further establish this model, more work with female animals and various age groups need to be performed, as well as studies to further establish and standardize methodologies for validation of the models for clinical relevance. Common data elements to standardize the reporting methodology for the CHIMERA literature are suggested.

1. Introduction

With long-term economic and medical repercussions, traumatic brain injury (TBI) is a current and growing global concern (James et al., 2019; Te Ao et al., 2014). Recent analysis of data from the *Global Burden of Diseases, Injuries, and Risk Factors 2016 Study* revealed there were about 27 million new cases of TBI in 2016 alone and an overall 8.4 percent increase in TBI prevalence over a span of 26 years (James et al.,

Table 1
Summary of parameters employed in CHIMERA studies.

Reference	Treatment variables							Morbidity
	Species	Sex	Age	Analgesia	Anesthesia[a]	Injury site	Injury parameters	
Bashir et al. (2020)	C57BL6 Mice	Females and males	5–7 months	1 mg/kg Meloxicam	5%/2–4% Isoflurane	Bregma	1 × 2.5 J with polylactic acid (PLA) interface	80%, shortly after CHIMERA
Chen et al. (2017)	C57Bl/6	Male	3 months	Not reported	5% Isoflurane	Bregma	3 × 0.6 J, 24-h intervals	No mortality
Cheng et al. (2018)	C57Bl/6 & APP/PS1 Mice	Males	~5.7 months	1 mg/kg Meloxicam	5%/4–5% Isoflurane	Midline parietal	2 × 0.5 J, 24-h interval	Not reported
Cheng et al. (2019)	C57Bl/6 & APP/PS1 Mice	Males	6 & 13 months	1 mg/kg Meloxicam	5%/4–5% Isoflurane	Midline parietal	2 × 0.5 J, 24-h interval	No mortality reported immediately after injury; 5 CHIMERA + 5 sham died in the 7 months following injury
Desai et al. (2020)	C57BL/6NCr Mice	Not reported	4–5 months	Not reported	5% Isoflurane	Bregma	Single: 1 × 0.55J Repeat: 3 × 0.55J, 24-h interval	Not reported
Gangolli et al. (2019)	C57Bl/6 & hTau Mice	Males	1–2 months	Not reported	5%/2.5% Isoflurane	Midline	20 × 0.13 J or 0.24 J, 24-h intervals	No mortality reported immediately after injury; 1-year survival ~ 10% deaths for hTau sham 0 deaths for 20 × 0.13 J CHIMERA ~ 25% deaths for 20 × 0.24 J CHIMERA
Haber et al. (2017)	C57Bl/6	Males	4 months	Not reported	4.5%/5% Isoflurane	Vertex of head	2 × 0.5 J or 0.65 J, 24-h interval	Not reported
Komlosh et al. (2018)	C57Bl/6N	Males	Not reported	Not reported	Not reported	Not reported	3 × 0.5 J, 24-h interval	Not reported
Krukowski et al. (2020)	C57BL/6J	Females & males	8–10 weeks old	Not reported	2–2.5% Isoflurane	Bregma	5 × 0.5 J, 24 h intervals	Not reported
Li et al. (2020)	C57Bl/6	Not reported	16–20 weeks old	Not reported	2.5–3% Isoflurane	Bregma	1 × 0.5–0.8 J or 2 × 0.5 J, 24 h intervals	Not reported
McInnes et al. (2020)	C57Bl/6 (Cadavers)	Male	8 months	n/a	n/a	Bregma	1–10 × 0.7 J	(Cadaveric mice)
Namjoshi et al. (2014)	C57Bl/6	Males	~4.3 months	1 mg/kg Meloxicam	5%/2.5–3% Isoflurane	Bregma	2 × 0.5 J, 24-h interval	~ 3% euthanized due to righting reflex > 45 min or severe motor dysfunction
Namjoshi et al. (2016)	C57Bl/6	Males	~4 months	1 mg/kg Meloxicam	5%/2.5–3% Isoflurane	Bregma	2 × 0.5 J, 24-h interval	Not reported
Namjoshi et al. (2017)	C57Bl/6	Males	4–5 months	1 mg/kg Meloxicam	5%/2.5–3% Isoflurane	Bregma	1 × 0.1–0.7 J	Not reported; skull fractures at energy levels > 0.7 J
Nolan et al. (2018)	C57Bl/6J	Males	2 months	Not reported	2% isoflurane	Bregma	5 × 0.5 J, 24-h interval	No mortality
Sauerbeck et al. (2018)	C57Bl/6J	Females & males	4 months	Not reported	5%/2.5% Isoflurane	4 mm posterior to the lateral canthus of eye	modCHIMERA, 1 × 1.7 J or 2.1 J Skull protected helmet/cradle reduced spine flexion	Mortality – 8.8% at 1.7 J and 23.4% at 2.1 J
Sauerbeck et al. (2020)	C57Bl/6J and APPswe/PSEN1dE9 mice	Males	~4 month old C57 mice; 18 month old APP mices	Not reported	Isoflurane	4 mm posterior to the lateral canthus of eye	modCHIMERA, 1 × 2.1 J Skull protected helmet/cradle reduced spine flexion	Mortality – 8%
Vonder Haar et al. (2019)	Long Evans Rats	Males	3 months	5 mg/kg Meloxicam	5%/2% Isoflurane	Anterior to bregma	1 × 2.9 J, 4 × 2.4 J, 2-week intervals	33% (8/24), 4 deaths on the first day (2.9 J), 4 more on subsequent 4 injuries (2.4 J)
Whyte et al. (2019)	Ferrets	Males	5–6 months	0.2 mg/kg Meloxicam	Isoflurane, 6 mg/kg Ketamine, 1 mg/kg Midazolam	Dorsal skull surface with PLA interface	6–10 × 17–56 J	2/3 ferrets used; immediately euthanized after injuries

[a] All studies employed isoflurane as anesthesia. Cases where two levels of isoflurane are indicated, separated by a slash, refer to the use of a higher initial level of isoflurane followed by a maintenance level once the animal was unconscious.

2019). Although TBI is underreported, global population growth, longer life expectancy, and the increase in transportation-related injuries indicate that the prevalence of TBI will continue to rise (James et al., 2019). The majority of TBI cases are mild injuries, most frequently associated with falls, motor vehicle accidents, and impact injuries, and significant proportions are sustained by very young children, adolescents, and older adults (Faul et al., 2010; James et al., 2019). Epidemiological studies and the Centers for Disease Control and Prevention's *Heads Up* campaign recognize the recent concerns regarding younger populations where there is a high incidence of mild TBI (mTBI) in young children and adolescents often related to sports-induced trauma (Coronado et al., 2015; Zhang et al., 2016). TBI is also common in the military, and is considered both the invisible wound and signature injury of modern warfare (Defense and Veterans Brain Injury Center, 2019; U.S. Department of Defense, 2019).

2. Clinical relevance of impact-rotational acceleration models

Broadly, TBIs can be caused by a focal, direct load to the head that induces injury from an impact, or by inertial forces from rapid head displacement that can lead to more diffuse pathology (Gennarelli, 1994; LaPlaca et al., 2007). For pre-clinical studies, one can further subdivide the mechanical input from impact injuries into models that apply a mechanical force to the skull or scalp—closed head injuries—or procedures that open the skull and produce direct injury by meningeal or brain deformation (Lighthall et al., 1989). Pre-clinical open-head injury models, primarily controlled cortical impact (CCI) (Lighthall, 1988) and fluid percussion injury (FPI) (Dixon et al., 1987) models, are reproducible and have provided valuable information regarding the mechanisms of TBI-related local cellular and axonal injuries. However, models that inflict focal damage and employ a fixed head approach with significant skull and cerebral deformation or penetration do not mimic the injury processes of the majority of human cases. Further, skull fractures, focal contusions, and high impacts to the head are associated with serious morbidity and death, but clinical TBI cases are more often associated with lesser degrees of focal injury and no conspicuous cerebral pathology. In these cases, skull durability protects brain tissue from focal contusion and fracture, but the impact causes rapid inertial changes in head velocity.

Neuropathological data, imaging, and simulation studies suggest high velocity head displacement leads to diffuse axonal injury from the significant strain the brain sustains from linear and rotational acceleration and deceleration during impacts (Cullen et al., 2016; Margulies and Thibault, 1992; Marmarou et al., 1994). Several models have been employed for direct, closed-head, load injuries, with wide applications of weight drop (Kilbourne et al., 2009) and a few controlled cortical impact models with unrestrained head movement (Bodnar et al., 2019; Jamnia et al., 2017; Petraglia et al., 2014; Prins et al., 2010), where inertial forces are thought to be a significant component of the injury process. Historically, these models also include the Maryland steel ball model of impact (Kilbourne et al., 2009), reflex hammer designs (Henry et al., 1997), or blast-induced trauma (Sawyer et al., 2016). Models, such as the spring-loaded Medical College of Wisconsin Rotational Injury device (Fijalkowski et al., 2007), where the impact allows for head movement, resulting in rapid velocity changes, have also been introduced. Pre-clinical models of impact acceleration have a long history and have included various animal species (see extensive references in (Gennarelli, 1994; Goldsmith, 2001; Goldsmith and Monson, 2005)). These earlier studies laid the groundwork for the later models, and importantly demonstrated that injury severity is associated with increases in the magnitude and duration of acceleration, with rotational acceleration thought to be the predominant component (Gennarelli et al., 1982; Hardy et al., 2001; Holbourn, 1943; LaPlaca et al., 2007; Mychasiuk et al., 2016; Ommaya et al., 1966; Rowson et al., 2012).
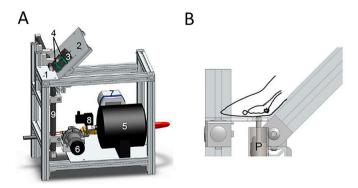
Due to its relevance to the major forms of trauma—falls, vehicular accidents, sports-related collisions—the present review focuses upon a relatively recent development in modeling impact acceleration effects: the Closed-Head Impact Model of Engineered Rotational Acceleration (CHIMERA) design created by Namjoshi and colleagues at the University of British Columbia, Canada (Namjoshi et al., 2014). The importance of this model relates to the commercial availability of the device, where investigators have the opportunity to standardize injury parameters; permitting replication across laboratories and further synthesis of the mechanisms of injury. In addition, devices have been designed for mouse, rat, and ferret; permitting eventual comparisons across these commonly used laboratory animal models. The review provides a status at this opportune time with the "milestone" publication of just fewer than 20 CHIMERA manuscripts (Table 1) that provide preliminary findings from this approach. Pathological findings are reviewed, obtained by traditional histochemical and neurophysiological methods, imaging, and functional outcomes evaluated by behavioral testing. This will be followed by a critical assessment of what needs to be accomplished for establishing research standards for this new model in pre-clinical studies of TBI, including suggested parameters to include when reporting common data elements.

3. CHIMERA operation and biomechanics

As noted, there are three CHIMERA devices that are scaled for use with mouse, rat, and ferret. The design embodies injuries that arise from an impact and resultant high velocity movement of the head and upper torso. For the mouse CHIMERA (Fig. 1), the combined compressive contact and inertial forces and the change in velocity and angular velocity stemming from the CHIMERA, after scaling, were reported as similar to pro-football and pro-boxing values, respectively (Namjoshi et al., 2014). Further tracking studies are warranted for all three devices with utilization of marker devices that allow more reliable and accurate estimation of head kinematics (see, e.g., (McInnes et al., 2020; Whyte et al., 2019)).

The CHIMERA devices deliver a high pressure-driven impact from a metal piston (labeled P in Fig. 1B) that strikes the dorsal surface of the head. Animals are secured in a supine position on the platform (3 in Fig. 1A) with Velcro straps (4 in Fig. 1A) that hold the animal in place after impact, and the user employs crosshairs demarcated on the device to position the head. An air compressor (not shown) is used to pressurize a storage tank (5 in Fig. 1A) and the animal's head is driven upward by the release of compressed air that mobilizes the piston located in a barrel below the platform. The release of the piston and

Fig. 1. Representations of the mouse CHIMERA device. A provides a basic depiction of the components of the mouse CHIMERA device. A mouse (shown in B) is secured by Velcro straps to the head plate (1 in A) so that while secured in the supine position a steel rod located in a piston barrel (9 in A and also shown in B) strikes the top surface of the scalp at high velocity. Crosshair marking (not seen) allows the investigator to align the head. The piston is driven toward the scalp by the release of a highly compressed air release from a storage tank (5 in A) that is electronically released by a solenoid valve (8 in A). An air pressure regulator (6 in A) allows for regulation of the air pressure that drives the piston. Figure from Namjoshi et al., 2014, used with permission.

velocity of the piston is regulated by an air pressure regulator valve (6 in Fig. 1A) located at the distal end of the air storage tank. A pressure gauge (7 in Fig. 1A) allows the investigator to regulate the amount of air released to control the level of impact. Two infrared photo-coupled devices measure the velocity of the piston just before impact, where velocity can be related to impact energy, measured in Joules (J). A user interface tablet with software triggers the device and records the measured velocity and pressure setting.

Table 1 provides an overview of the parameters employed in publications that have utilized a CHIMERA device. Seventeen of the 19 published reports employed the laboratory mouse and with the exception of the two studies by Cheng and colleagues, younger mice were the test subjects. For the studies that reported the sex of the mice, all studies, with the exception of Sauerbeck, et al., Bashir and coworkers, and Krukowski and colleagues, tested male mice exclusively (Sauerbeck et al., 2018; Bashir et al., 2020; Krukowski et al., 2020). The single recent study by Vonder Haar that used rats likewise employed males only (Vonder Haar et al., 2019). The typical energy used in the mouse studies was 0.5 J, but one group (Chen et al., 2017; Desai et al., 2020) increased the energy to 0.55–0.6 J, and a recent publication employed a range up to 0.8 J (Li et al., 2020). Others have employed higher energy settings (1.7–2.5 J) in mice with the addition of an interface to reduce focal contusions (Bashir et al., 2020; Sauerbeck et al., 2018; Sauerbeck et al., 2020). The modCHIMERA used by Sauerbeck and colleagues includes both a helmet and body cradle, constructed with flexible Tygon tubing, which altered the injury trajectory of the animal since the cradle restricted torso and head movement (Sauerbeck et al., 2018). Bashir and coworkers utilized a polylactic acid (PLA) interface lined with cured putty that matched the contour of the mouse's head, covering the lower part of the skull (Bashir et al., 2020). Namjoshi, et al. examined pathological effects over a range of energy levels (0.1–0.7 J), and designated 0.5 J as the "threshold" for concussive injury, leading to a significant change from one or more phenotype (Namjoshi et al., 2017). The majority of studies in mice are designed with a 0.5 J energy level with multiple impacts distributed once a day. Vonder Haar and colleagues utilized higher energy levels (2.4–2.9 J) in their rat studies (Vonder Haar et al., 2019). In the one study to date employing ferrets, energy levels of 17–56 J were employed with the addition of a PLA interface on the head of the animal (Whyte et al., 2019).

4. Pathological changes

Sports- and motor vehicle-related TBI frequently involve high-rate head acceleration (Rowson et al., 2012; Stemper et al., 2015), which causes pathological changes in the brain that are distinct from those of a direct localized impact to the head. This type of injury affects major white matter tracts, which are thought to be damaged when they undergo shearing forces characteristic of rotational acceleration. Inflammation results from this type of damage and can persist for a long time after the initial insult (Johnson et al., 2013). Current studies using CHIMERA outline these major changes after injury, as well as additional subtle changes in the accumulation of misfolded proteins, receptor expression, and neuronal death.

4.1. Axonal injury

As noted, a main pathological feature of rotational closed-head injury is damage to major axonal pathways (Table 2). Axonal damage in the acute phase can be visualized using immunohistochemistry for neurofilament (NF), a cytoskeletal protein, or amyloid precursor protein (APP). Damage causes these proteins to accumulate in neuronal processes as a result of disruption to axonal transport, giving axons the appearance of swellings or bulbs. The staining is transient as the disruption of cell trafficking resolves or damaged elements are removed from the tissue. As summarized below, more long-term damage to axons was identified by silver staining techniques.

Antibody staining for components of NF can also reveal the integrity of axons after injury. Seven days after injury (2 × 0.5 J or 0.65 J, 24-h interval), Haber and colleagues, using a pan-NF antibody, observed many retraction bulbs and axonal varicosities in the optic tracts of injured mice (Haber et al., 2017). Likewise, Komlosh and others, using an antibody for NF light-chain, found that 7 days after injury (3 × 0.5 J, 24-h intervals) the optic tracts showed increased axonal varicosities compared to the uninjured animal (Komlosh et al., 2018). Another group found that axonal swellings were increased in the optic tracts of injured APP/PS1 and wild-type mice at 2 days (2 × 0.5 J, 24-h interval), but the swellings had disappeared by 7 days after the last injury (Cheng et al., 2018). An increase in NF light-chain was also observed in the plasma of injured APP/PS1 mice by ELISA at 2 days following injuries, but was not present in any other group (sham APP/PS1 or wild-type mice) and was no longer evident in the injured APP/PS1 mice by 7 days after injuries (Cheng et al., 2018). One day after modified CHIMERA (modCHIMERA; 1 × 1.7 J or 2.1 J with helmet), an increased density of puncta was qualitatively observed, compared to sham animals, in the corpus callosum, anterior commissure, hippocampal commissure, and fimbria using an antibody for phosphorylated NF heavy-chain (Sauerbeck et al., 2018). Other studies report that at later time points axonal varicosities and retraction bulbs are no longer evident, as no differences between injured and sham animals were reported in NF light-chain staining 3 weeks after injury (1 × 2.9 J followed by 4 × 2.4 J, 14 day intervals; rats) or in NF medium- and heavy-chain staining 8 months after injury (2 × 0.5 J, 24-h interval; mice) in the corpus callosum and optic tracts of mice and rats (Cheng et al., 2019; Vonder Haar et al., 2019). Staining with NF is greater in injured animals within the first week, but is no longer evident past 7 days, possibly due to cell repair mechanisms or death of affected neurons.

In two separate studies, at 7 days after injury (2 × 0.5 J, 24-h interval and 2 × 0.5 J or 0.65 J, 24-h interval), immunocytochemistry of major white matter tracts showed no APP staining (Haber et al., 2017; Namjoshi et al., 2016). In another study, increased staining was seen one and 7 days after injury (3 × 0.6 J, 24-h intervals) in the corpus callosum but returned to sham levels by 1 month (Chen et al., 2017). A study that measured puncta of β-APP in major white matter tracts 1 day after two injury levels (modCHIMERA; 1 × 1.7 J or 2.1 J with helmet) found an increase in density of APP in the corpus callosum at both injury levels, in the anterior commissure at the higher injury level, and a dose-dependent increase, compared to sham, in the hippocampal commissure and fimbria (Sauerbeck et al., 2018). The most recent study to look at APP staining in white matter tracts found no changes after injury (1 × 2.5 J with PLA interface) at any of the acute or chronic time points tested (6 h, 2 days, 2 weeks, 1 and 2 months) in either the optic tract or corpus callosum (Bashir et al., 2020). To date, no study has employed the CLARITY procedure to identify axonal injury after CHIMERA TBI. A recent study that employed the CCI model in mice reported that CLARITY staining detected axonal bulb profiles 1 month after CCI, and that there was evidence the bulbs retained distal processes (Weber et al., 2019). Application of this method may reveal information about the pattern of axonal injury following CHIMERA that is not found by traditional immunohistochemistry.

While NF and APP accumulation may be cleared by 7 days post-injury, silver staining reportedly shows changes in white matter tracts for a longer time after the initial injury. Namjoshi and others found greater silver uptake in the corpus callosum and optic tracts two, seven, and 14 days after injury (2 × 0.5 J, 24-h interval), with a progressive increase in silver uptake in the optic tracts (Namjoshi et al., 2014). In a later study, the same group found increased silver uptake at 7 days post injury (2 × 0.5 J, 24-h interval) in the corpus callosum, external capsule, and optic tracts (Namjoshi et al., 2016). When comparing different levels of injury categorized as sub-threshold (1 × 0.1, 0.3, or 0.4 J), threshold (1 × 0.5 J), and mild TBI (1 × 0.6 or 0.7 J), increased silver stain was detected in the corpus callosum only in the mTBI group by day two and remained elevated on day 14. The optic tracts showed

Table 2
Axonal neuropathology after CHIMERA injuries.

Time following injury	Method	Findings	Injury parameters	Reference
2, 7, 14 days	Silver stain	Increased silver uptake in OLF at 2 days, back to baseline by 7 days; increased in CC at 2–14 days; increased in OPT at 2 days and continued to increase by 14 days	2 × 0.5 J, 24-h interval	Namjoshi et al. (2014)
7 days	Silver stain & APP	Increased silver uptake in CC, OPT, and external capsule; no APP detected in white matter tracts	2 × 0.5 J, 24-h interval	Namjoshi et al. (2016)
1, 7 days; 1 month	APP	Increased in CC at 1 and 7 days, back to baseline by 1 month	3 × 0.6 J, 24-h intervals	Chen et al. (2017)
7 days	APP, MBP, NF	No change in APP; slight increase in MBP but not significant; NF retraction bulbs present in TBI but not sham	2 × 0.5 J or 0.65 J, 24-h interval	Haber et al. (2017)
6 h; 1, 2, 7, 14 days	Silver stain	Increased in OLF after 1 and 2 days, returns to baseline by 7 days; increased in CC after 2 days and remains elevated; increased in OPT after 2 days in threshold and mTBI groups, returns to baseline in threshold but remains elevated by 14 days in mTBI group	1 × 0.1–0.7 J	Namjoshi et al. (2017)
2, 7, 14 days	NeuroSilver stain, NF-M and NF-H	Increased silver uptake at 14 days in both WT and APP/PS1 injured; increased axonal swelling after 2 days in OPT, returns to baseline by 7 days; higher plasma concentration of NF-M/-H in 6.1-month-old APP/PS1 injured mice at 2 days	2 × 0.5 J, 24-h interval	Cheng et al. (2018)
7 days	NF-L	Axonal varicosities present in injured but not sham	3 × 0.5 J, 24-h interval	Komlosh et al. (2018)
1 day	APP, phosphorylated NF-H	APP positive puncta increased in CC at both levels of injury, in anterior commissure only at 2.1 J, and in HP commissure and fimbria at both injury levels in dose-dependent manner; NF-H positive puncta observed but not quantified in CC, anterior commissure, HP commissure, and fimbria	modCHIMERA, 1 × 1.7 J or 2.1 J	Sauerbeck et al. (2018)
8 months	NeuroSilver, NF-M and NF-H, APP	Increased NeuroSilver stain in OPT; no changes observed in NF or APP in OPT or CC	2 × 0.5 J, 24-h interval	Cheng et al. (2019)
1 year	Myelin Black Gold II	Decreased power coherence in CC, HP commissure, and fimbria after injury; power coherence was more reduced in 0.24 J group vs 0.13 J	20 × 0.13 J or 0.24 J, 24-h intervals	Gangolli et al. (2019)
3 weeks	Silver stain, NF-L	Increased silver uptake in OPT; no change in NF-L count in CC or OPT, but CC was thinner after injury	1 × 2.9 J, 4 × 2.4 J, 2-week intervals	Vonder Haar et al. (2019)
5 weeks	Silver stain	Significantly increased silver uptake in optic tract of repeated injury mice	Single: 1 × 0.55J Repeat: 3 × 0.55J, 24-h interval	Desai et al. (2020)
6 h, 2, 14, 30, 60 days	Silver stain & APP	No change in % area APP in OPT or CC; elevated silver uptake in OPT at 14, 30, and 60 days post injury; no change in silver uptake in CC	1 × 2.5J, with PLA interface	Bashir et al. (2020)

Abbreviations. APP: amyloid precursor protein; CC: corpus callosum; CTX: cortex; HP: hippocampus; MBP: myelin basic protein; NF: neurofilament (-L: light; -M: medium; -H: heavy); OLF: olfactory nerve layer of olfactory bulb; OPT: optic tracts; PFC: prefrontal cortex; PLA: polylactic acid WT: wild-type

increased staining in both the threshold and mTBI groups by 2 and 7 days but remained elevated only in the mTBI group 2 weeks after injury. Axonal damage measured by silver uptake in the olfactory nerve layer of the olfactory bulb was only seen in the mTBI group one and 2 days after injury, but by 7 days had disappeared (Namjoshi et al., 2017). A qualitative study showed greater silver uptake in the optic tract of mice 5 weeks after repeat CHIMERA (3 × 0.55 J, 24-h interval) compared to single (1 × 0.55 J) or sham injured mice (Desai et al., 2020). Bashir and colleagues measured the percent area stained by silver uptake at both acute and chronic time points in the optic tract and corpus callosum after a greater level of injury (1 × 2.5 J with PLA interface). Similar to some previous studies, they found no changes in the corpus callosum. The optic tract showed no changes in silver uptake acutely at 6 h or 2 days, but did show elevated uptake from 2 weeks that remained up to 2 months after injury (Bashir et al., 2020).

A study comparing wild-type mice to APP/PS1 mice found an increase in silver uptake 14 days after injury (2 × 0.5 J, 24-h interval) in the optic tracts of both wild-type and transgenic mice (Cheng et al., 2018). The same group found that silver uptake was increased in the optic tracts up to 8 months after injury (2 × 0.5 J, 24-h interval), but found no difference in the corpus callosum between the TBI and sham groups (Cheng et al., 2019). Another group found increased silver uptake in the optic tracts of rats 3 weeks after injury (1 × 2.9 J followed by 4 × 2.4 J, 14 day intervals), but no change in the corpus callosum (Vonder Haar et al., 2019). Overall, silver staining shows damage to axons at more chronic time points and appears consistently in the optic tracts at later time points following injury by CHIMERA. Other white matter tracts, such as the corpus callosum, may also show damage by silver staining, but this result is not consistent across the studies reviewed here.

Insults to white matter tracts can result in demyelination, which leaves exposed axons vulnerable to further damage (Armstrong et al., 2016). Myelination can be measured by quantifying changes in myelin basic protein (MBP), a major component of the myelin sheath. One study measured MBP 7 days after injury (2 × 0.5 J or 0.65 J, 24-h interval) and observed a slight, but non-significant increase in MBP in the injured group compared to sham, indicating changes in myelin that were also seen as diffusion tensor imaging (DTI) abnormality (Haber et al., 2017). Another group measured white matter integrity by employing power coherence analysis of Myelin Black Gold II stained images 1 year after injury (20 × 0.13 J or 0.24 J, 24-h intervals) and found that integrity of the white matter was reduced in the corpus callosum, hippocampal commissure, and fimbria compared to sham. The reduction was greater for the concussive (0.24 J) than the sub-concussive (0.13 J) injury (Gangolli et al., 2019). Myelin plays a complicated role in axon pathology and repair. While it is thought that myelin may protect axons from damage, the presence of myelin debris can also inhibit axon regeneration (Armstrong et al., 2016). Further work remains to be done to characterize possible changes in myelination acutely and chronically in the CHIMERA model, and the implications this may have for chronic white matter pathology and axon regeneration.

Initial axonal injury from TBI may result from primary or secondary injury pathways and may either resolve spontaneously or may proceed to Wallerian degeneration, in which the axon degrades entirely. Thus, some axons that initially display impaired axonal transport (APP puncta) may repair the damage, while others appear as degenerating axons at later time points. The existence of a period of time after injury during which axonal damage can be prevented or reversed creates a therapeutic window in which treatments for mild TBI can be tested (Armstrong et al., 2016). Injury by CHIMERA consistently shows both acute and chronic damage to white matter tracts (summarized in Table 2), a pattern of diffuse axonal injury that resembles that seen in human TBI (Johnson et al., 2012), making CHIMERA a promising preclinical model for this therapeutic window during which additional degeneration can be halted or repair mechanisms initiated.

4.2. Amyloid beta and tau

A history of traumatic brain injury has been linked to later development of Alzheimer's disease (AD) (Fleminger et al., 2003), which is characterized by pathologic accumulation of amyloid beta (Aβ) plaques and tau protein neurofibrillary tangles. In a model of AD using APP/PS1 mice expressing the human APP transgene, Cheng and others found that Aβ deposits were increased in younger (6.1 months) mice 2 days after injury (2 × 0.5 J, 24-h interval), and had resolved by 7 days; they observed no change in Aβ deposits in the older mice (13.5 months) at any time point (Cheng et al., 2018). In contrast, Thio-S staining for amyloid plaques revealed an increase in staining density in the older mice at 6 h followed by a decrease, compared to sham animals, by 2 and 7 days, and a return to sham levels by 14 days (Cheng et al., 2018). When the authors compared Aβ in whole brain homogenates via ELISA and Western blot, they found no difference in protein levels between sham and injured mice at any age or genotype (Cheng et al., 2018). In a second study, the same group found no change in carbonate-soluble/insoluble Aβ40 and Aβ42, and no change in diffuse/neuritic plaques by 8 months (Bashir et al., 2020). However, an aducanumab binding assay indicated that brain tissue from the injured APP/PS1 mice exhibited greater levels of higher molecular weight oligo/soluble Aβ fibrils (Cheng et al., 2019).

Tau is a microtubule-associated protein that has been linked with chronic traumatic encephalopathy (CTE), thought to result from repeated concussive or sub-concussive head injuries (Johnson et al., 2012; McKee et al., 2009). When three phosphorylation sites for tau were probed acutely after two injuries (2 × 0.5 J, 24-h interval), phosphorylation at all sites was increased at 6 h, 12 h, and 2 days, and the authors found an increased ratio of phosphorylated-to-total tau in the injured mice (Namjoshi et al., 2014). When animals sustained a single injury (1 × 0.1–0.7 J) and levels of total and phosphorylated tau were probed from 6 h to 14 days, no changes were observed (Namjoshi et al., 2017). However, a later study measuring tau phosphorylation in brain lysates with the same antibodies found no difference in phosphorylation 7 days after two injuries (2 × 0.5 J, 24-h interval) (Namjoshi et al., 2016). Western blot of brain homogenates performed 6.5 months after a repetitive injury (3 × 0.6 J, 24-h intervals) revealed no change in tau expression in the cortex or hippocampus (Chen et al., 2017). Following a single, moderate injury using a PLA interface (1 × 2.5 J), Bashir and colleagues observed an increase in total tau, phosphorylated tau, and in the ratio of phosphorylated tau to total tau at 6 h and an increase in total tau at 14 days following injury in brain homogenates. All measures of tau returned to sham levels by 30 and 60 days (Bashir et al., 2020). Immunohistochemistry for phosphorylated tau showed a group effect of injury compared to sham in the entorhinal cortex, but no differences in the CA1 region of the hippocampus, nor in the optic tract or corpus callosum (Bashir et al., 2020).

In APP/PS1 transgenic mice, Cheng and colleagues found that repeated injury (2 × 0.5 J, 24-h interval) did not change tau expression in young (6.1 months) or old (13.5 months) mice at either 6 h or 2 days after injury (Cheng et al., 2018), in contrast with previous findings of increased tau phosphorylation at acute time points (Namjoshi et al., 2014). Similarly, a transgenic mouse model expressing human tau (hTau) did not show any tau pathology in the hippocampus at a chronic time point of 1 year following a repetitive sub-concussive or concussive injury (20 × 0.13 J or 0.24 J, 24-h intervals) (Gangolli et al., 2019). However, a model using male Long-Evans rats found that 3 weeks after injury (1 × 2.9 J followed by 4 × 2.4 J, 14 day intervals), phosphorylated tau was increased in the optic tract and qualitatively increased in the nucleus accumbens and orbitofrontal cortex, but total tau was not changed by injury (Vonder Haar et al., 2019). While increasingly being studied in the context of brain injury, it is still unclear how the timing, intensity, and preclinical model of injury play a role in tau pathology, and the implications this has for the long-term consequences of TBI.

Table 3
Neuroinflammation after CHIMERA injuries.

Time following injury	Microglia pathology	Astrocyte pathology	Injury parameters	Reference
2, 7, 14 days	Greater number and more activated cells in CC, brachium of superior colliculus, OLF, OPT	n/a	2 × 0.5 J, 24-h interval	Namjoshi et al. (2014)
7 days	Greater number and more activated cells in CC, brachium of superior colliculus, OLF, OPT	n/a	2 × 0.5 J, 24-h interval	Namjoshi et al. (2016)
1, 7 days; 3.5, 6.5 months	Increased number of activated cells after 1 day in OPT, CC, CTX, and HP; in OPT remain activated at 3.5 months and return to 1 day level by 6.5 months	Increased at 1 day, 3.5, & 6.5 months in OPT; increased only at 1 day in CC, HP, CTX	3 × 0.6 J, 24-h intervals	Chen et al. (2017)
7 days	Increased % area stained in brachium of superior colliculus	Increased % area stained in brachium of superior colliculus and OPT	2 × 0.5 J or 0.65 J, 24-h interval	Haber et al. (2017)
6 h; 1, 2, 7, 14 days	Increased cell number in CC, brachium of superior colliculus, OPT from 2 to 14 days in sub-threshold, threshold, and mTBI groups; increased in OLF at 1 day in mTBI, 2–14 days in all injury levels	Increased in threshold and mTBI after 2 days; increased in mTBI after 7 days and back to baseline by 14 days	1 × 0.1–0.7 J	Namjoshi et al. (2017)
2, 7 days	Increased cell density in OPT at 7 days in 13.5-month-old WT and 6.1-month-old APP/PS1; Mean cell size greater in APP/PS1 6.1-month-old mTBI mice	n/a	2 × 0.5 J, 24-h interval	Cheng et al. (2018)
36–40 days	Increased cell density in layers II-VI of medial PFC and in CA1 of HP	No change in CA1 of HP in injured mice	5 × 0.5 J, 24-h interval	Nolan et al. (2018)
1 month	Dose-dependent increased cell density in lateral septal nucleus, CTX, HP	n/a	modCHIMERA, 1 × 1.7 J or 2.1 J	Sauerbeck et al. (2018)
8 months	Increased cell density & size in OPT; increased total cells and activated microglia in PFC of APP/PS1 injured; more activated microglia in amygdala of APP/PS1 sham but reduced after injury; increase in non-activated microglia in HP of APP/PS1 sham but decreased after injury	Increased in OPT after TBI; increased in APP/PS1 compared to WT in PFC, amygdala, and HP but no effect of injury	2 × 0.5 J, 24-h interval	Cheng et al. (2019)
1 year	Increased % positive staining in CC after 0.24 J, but not after 0.13 J	No change in % area stained in CTX, HP, anterior commissure, fimbria, lateral septal nucleus, CC, or HP commissure	20 × 0.13 J or 0.24 J, 24-h intervals	Gangolli et al. (2019)
3 weeks	Increased cell count in CC, OPT, and olfactory tubercle	Increased cell count in CC	1 × 2.9 J, 4 × 2.4 J, 2-week intervals	Vonder Haar et al. (2019)
5 weeks	Increased mean fluorescence intensity in OPT after repeated injury	Progressively increased mean fluorescence intensity in OPT between single and repeat injury	Single: 1 × 0.55J Repeat: 3 × 0.55J, 24-h interval	Desai et al. (2020)
6 h, 2, 14, 30, 60 days	Increased % area stained in entorhinal cortex at 6 h and 2 days, returns to sham level by 14 days; elevated in CA1 of HP at 2 days; elevated in OPT at 14 and 60 days; no change in CC	Group effect of injury in entorhinal cortex; increased % area stained in OPT at 60 days; no change in CC or CA1 of HP	1 × 2.5J, with PLA interface	Bashir et al. (2020)
3 days	Increased number in OPT	Increased in CA1 and CC	1 × 0.8 J	Li et al. (2020)

Abbreviations. CA1: cornu Ammonis field 1 of the hippocampus; CC: corpus callosum; CTX: cortex; HP: hippocampus; OLF: olfactory nerve layer of olfactory bulb; OPT: optic tracts; PFC: prefrontal cortex; PLA: polylactic acid; WT: wild-type

4.3. Inflammation

Inflammation after traumatic brain injury has been characterized in animal models as well as in clinical populations (Corps et al., 2015; Frugier et al., 2010). The main effectors of the inflammatory response after injury are microglia and astrocytes. Microglia are the resident immune cells of the brain and can be found throughout the parenchyma. In normal conditions, microglia exist in a ramified state, with multiple branched projections that constantly surveil the extracellular environment. When they are activated by injury or disease, they adopt a hyper-ramified "bushy" or amoeboid morphology and release cytokines and chemokines. In the amoeboid morphology they can travel to the site of injury and phagocytose dying cells and cellular debris. Astrocytes function normally to support neuronal function and become reactive and proliferative in response to injury or disease.

Initial characterization of the CHIMERA model (Table 3) evaluated microglial number and morphology in the major white matter tracts at two, seven, and 14 days post injury (2 × 0.5 J, 24-h interval) and found that the number of microglia was significantly increased in the corpus callosum, brachium of the superior colliculus, olfactory nerve layer, and optic tracts in the injured group compared to sham animals (Namjoshi et al., 2014). Additionally, microglia in these regions were activated, displaying a bushy, hypertrophic morphology compared to sham animals. In the optic tracts, microglia adopted an amoeboid, highly activated morphology, and the number of cells increased from 2 days to 14 days post-injury (Namjoshi et al., 2014). In a study with identical injury parameters where microglia were evaluated in major white matter tracts 7 days after the last injury, fractal analysis of cell morphology showed again that microglia in all tracts were less ramified and more amoeboid, compared to microglia in the sham-treated mice (Namjoshi et al., 2016).

A later study with similar injury (2 × 0.5 J or 0.65 J, 24-h interval) found increased microglia only in the brachium of the superior colliculus after 7 days, and increased glial fibrillary acidic protein (GFAP) expression in the brachium of the superior colliculus and the optic tracts (Haber et al., 2017), indicating that the inflammatory response after CHIMERA injury is supported by astrocytes as well as microglia. By 5 weeks, Desai and others found greater mean fluorescence of both astrocytes and microglia in the optic tracts after both single and repeated injury (1 × 0.55 J and 3 × 0.55 J, 24-h intervals). Chen and colleagues explored long-term inflammatory responses and found that the number of microglia was increased in the optic tracts, corpus callosum, hippocampus, and cortex 1 day after injury (3 × 0.6 J, 24-h intervals) and remained elevated at 6.5 months (Chen et al., 2017). In the optic tracts, microglial numbers peaked at 3.5 months, and in the hippocampus 7 days after injury (Chen et al., 2017), indicating that persistent microgliosis may follow a different profile depending on the region evaluated and the timespan after injury. In addition to microglial activation, reactive astrocytes were identified in the brains of injured animals. A two-fold increase in GFAP expression was seen in the optic tract, corpus callosum, hippocampus, and cortex 1 day after injury, and remained elevated in all regions at 6.5 months. In the optic tracts, GFAP expression increased three-fold compared to sham animals by 3.5 months and remained at that level at 6.5 months (Chen et al., 2017), indicating long-lasting activation of astrocytes after CHIMERA that does not resolve by 6 months.

Namjoshi and colleagues evaluated the effects of a range of different impact energies (1 × 0.1 to 0.7 J), which the authors binned into categories based on behavioral and pathological outcomes (Namjoshi et al., 2017). Impacts between 0.1 J and 0.4 J were considered sub-threshold, 0.5 J was considered threshold, and 0.6 or 0.7 J were classified as a mild TBI. Increased impact energy resulted in a greater number of microglia in four regions of interest: the olfactory nerve layer, corpus callosum, brachium of the superior colliculus, and the optic tracts. By 2 days after a single injury, the mTBI group showed greater numbers of microglia in all regions, which was sustained 14

days after injury. By contrast, a threshold injury only produced microgliosis in the olfactory nerve layer and corpus callosum 14 days post-injury, and in the brachium of the superior colliculus and optic tract at 2 days post-injury. Microglial numbers in the sub-threshold injury group were elevated only at 14 days after injury in the brachium of the superior colliculus and the optic tracts (Namjoshi et al., 2017). Likewise, the density of GFAP stained cells was increased in the threshold and mTBI groups at 2 days post-injury, remained elevated in the mTBI group at 7 days, and returned to sham levels in all groups by 14 days (Namjoshi et al., 2017). Mice subjected to a greater level of injury (1 × 2.5 J with PLA interface) showed greater staining of microglia in the optic tracts at 14 and 60 days, but not at two or 30 days, as well as greater astrocyte activation by 60 days (Bashir et al., 2020). The authors found no changes in inflammation in the corpus callosum at any time point.

A study investigating the effects of repetitive CHIMERA (20 × 0.13 J or 0.24 J, 24-h intervals) on 4-month-old hTau transgenic mice found no changes in astrocyte activation 1 year after the last injury, but did find increased numbers of microglia in the corpus callosum at 1 year (Gangolli et al., 2019). Another study using Long-Evans rats found microglia were increased in the corpus callosum, optic tracts, and the olfactory tubercle 3 weeks after injury (1 × 2.9 J followed by 4 × 2.4 J, 14 day intervals) as well as increased numbers of astrocytes in the corpus callosum, but not in the optic tracts (Vonder Haar et al., 2019). These results indicate that changes in inflammation are dependent on the extent of injury and that they may not appear immediately after impact.

The majority of studies have investigated the effects of CHIMERA in young mice (~4 months old). Cheng and others used older animals (6.1 and 13.5 months old) and compared C57BL/6-C3H wild-type male mice with APP/PS1 transgenic mice. After injury (2 × 0.5 J, 24-h interval), greater numbers of microglia were observed in the optic tracts of 13.5-month-old wild-type mice and of 6.1-month-old APP/PS1 mice on day seven after injury (Cheng et al., 2018). A later study from the same group found a greater number of microglia in the optic tracts 8 months after CHIMERA (2 × 0.5 J, 24-h interval) in both wild-type and APP/PS1 5.7-month-old mice (Cheng et al., 2019). Increased fluorescence intensity of GFAP was found 8 months after injury in the optic tracts of both cohorts of mice, suggesting that the optic tracts may be particularly vulnerable to long-lasting inflammation after TBI (Cheng et al., 2019).

While injury to white matter tracts is known to occur after a mTBI, inflammation can also be observed in gray matter regions. Namjoshi and colleagues observed an increase in Iba-1-positive microglia, 2 days after injury, in the lateral geniculate nucleus (Namjoshi et al., 2017). Nolan and colleagues found an increased cell density of microglia in the medial prefrontal cortex and the CA1 region of the hippocampus 36–40 days after injury (5 × 0.5 J, 24-h intervals), but no change in astrocyte activation in the hippocampus (Nolan et al., 2018). Sauerbeck and others used a modified injury protocol (modCHIMERA; 1 × 1.7 J or 2.1 J) and found an increase in cell density of microglia 1 month after injury in the lateral septal nucleus in a dose-dependent manner and in the entorhinal area/lateral cortex and hippocampus only after the higher injury level (Sauerbeck et al., 2018). Meanwhile, another group using a greater injury level (1 × 2.5 J with PLA interface) found greater microglia activation in the entorhinal cortex only at 6 h and 2 days, which returned to normal by 2 weeks. They found a main group effect of astrocyte activation in the same region, but individual time points were not significantly changed. The hippocampus in these mice showed greater microglial activation but no change in astrocyte staining in the injured group (Bashir et al., 2020). These findings, when paired with behavioral outcomes, indicate a mechanism by which changes in the brain may be leading to pathological changes in behavior (reviewed in Section 6 below).

Levels of cytokines and chemokines are expected to be upregulated after TBI (Corps et al., 2015; Frugier et al., 2010). Tumor necrosis factor

alpha (TNFα) and interleukin-1 beta (IL-1β) are expressed 2 days after injury (2 × 0.5 J, 24-h interval) as measured in brain lysates (Namjoshi et al., 2014). TNFα gene expression was also found to be increased in the cortex and hippocampus of injured (3 × 0.6 J, 24-h intervals) mice at 1 day post-injury and returned to sham levels by 3 days (Chen et al., 2017). Multiplex ELISA showed an increase 6 h after injury (1 × 0.1 - 0.7 J) of IL-6, IL-1β, and TNFα in brain lysates only in the mTBI group (0.6–0.7 J) compared to the sham, sub-threshold (0.1–0.4 J), and threshold (0.5 J) groups (Namjoshi et al., 2017). Use of a greater injury level (1 × 2.5 J with PLA interface) produced a similar cytokine profile compared to sham. IL-6, IL-1β, and TNFα were all elevated by 6 h following injury and while IL-6 and IL-1β returned to sham levels by 2 days, levels of TNFα took 2 weeks to return to sham levels (Bashir et al., 2020).

A study comparing APP/PS1 transgenic mice to wild type-mice found that IL-1β was upregulated only in the young (6.1-month-old) cohort of APP/PS1 mice 6 h after injury (2 × 0.5 J, 24-h interval), but not in the older (13.5-month-old) or wild-type cohorts (Cheng et al., 2018). In male Long-Evans rats, levels of IL-6, IL-1β, and TNFα were unchanged 3 weeks after injury (1 × 2.9 J followed by 4 × 2.4 J, 14 day intervals) as measured in the midbrain and forebrain (Vonder Haar et al., 2019). Based on these studies, changes in cytokine expression after CHIMERA appear acute and transient.

In summary, inflammation is a critical aftereffect of injury, and low-grade inflammation is thought to be a chronic long-term consequence of this type of injury (Johnson et al., 2013). Current studies using CHIMERA have found consistent changes in microglial density and activation, which appear to be most pronounced in major white matter tracts, although they can also be observed in gray matter such as cortex and hippocampus. These changes occur acutely by 1–2 days and can persist in some models up to 1 year following the last injury. Astrocyte activation, while less studied than microglia in the articles reviewed, was also observed to occur after some injuries produced by CHIMERA, mainly in the white matter tracts. Concurrent with other inflammatory changes, an acute but transient increase in cytokine expression has been shown to occur after CHIMERA.

4.4. Other pathology

Additional pathological markers of degeneration show that injury using CHIMERA can cause neurodegeneration while not resulting in obvious tissue deformation. Fluoro-Jade staining, a marker of neuronal death, after modCHIMERA (1 × 1.7 J or 2.1 J) showed positively stained cells in the hippocampus of the higher energy (2.1 J) group 1 day after the injuries, but no difference by 3 days, and no difference in staining in the cortex at either time point. These changes were not accompanied by any change in total cerebral volume (Sauerbeck et al., 2018). A study in rats found no change in Fluoro-Jade staining after injury (1 × 2.9 J followed by 4 × 2.4 J, 14 day intervals) in the ventral tegmental area (VTA) and olfactory tubercle at 3 weeks (Vonder Haar et al., 2019). Cresyl violet staining showed qualitative superficial injury after modCHIMERA (1 × 1.7 J or 2.1 J) at 1 month, along with immunoglobulin G (IgG) extravasation indicating permeability of the blood-brain barrier (BBB), and Perl's staining for iron deposits showing meningeal iron accumulation from microbleeds in the higher (2.1 J) energy level group (Sauerbeck et al., 2018). Likewise, another group using a greater injury level with a PLA interface (1 × 2.5 J) found greater IgG staining in the entorhinal cortex at 6 h (Bashir et al., 2020). The same group found elevated levels of tau and NF-L in the plasma 6 h following injury, as well as structural damage to the vasculature of the entorhinal cortex observed via electron microscopy, which are additional indications that the blood-brain barrier is compromised (Bashir et al., 2020). These findings prompt further investigation into subtle effects as well as potential changes in BBB permeability and vascular integrity after CHIMERA.

Mild TBI may cause changes in neuronal synaptic transmission (Bales et al., 2009). However, serotonin receptor expression measured by immunohistochemistry was not affected by injury (2 × 0.5 J, 24-h

interval) at 7 days (Namjoshi et al., 2016). An overall group effect of injury (1 × 2.5 J with PLA interface) was observed in staining for glutamatergic synapses in the CA1 region of the hippocampus (Bashir et al., 2020). Dopaminergic function measured by puncta of tyrosine hydroxylase showed no change after injury (1 × 2.9 J followed by 4 × 2.4 J, 14 day intervals) in rats, but a reduction of the dopamine transporter-to-tyrosine hydroxylase ratio was observed in the olfactory tubercle at 3 weeks (Vonder Haar et al., 2019). To date, only one study has compared overall changes in pre- and post-synaptic density in the CHIMERA model. The authors found that synaptic loci are reduced in the cortex by 7 days following injury (1 × 2.1 J) and remain lower up to 30 days after modCHIMERA (Sauerbeck, 2020). Electron microscopy in the L1 cortex of these mice confirms that the synapses exhibited structural damage at 7 days following injury (Sauerbeck, 2020). These results indicate that further study on the effects of CHIMERA on synaptic structure is warranted, particularly given the results from studies of changes in electrophysiological properties of neuronal networks (discussed in Neurophysiology section).

Unlike in open-skull models of TBI such as CCI or FPI, the pathological changes observed after injury by CHIMERA are more subtle. CCI and FPI result in loss of tissue with a clear cortical lesion and the formation of glial scars, particularly at chronic time points (Osier et al., 2015), whereas CHIMERA has not been shown to produce loss of tissue in the same way. Silver staining after CCI has shown degenerating neurons in the cortex and hippocampus and IgG extravasation indicated widespread breakdown of the BBB (Smith et al., 1995). CHIMERA results in silver uptake in various brain regions, and two studies looking at IgG extravasation have found BBB permeability, but only at higher energy levels using either a helmet or interface (Bashir et al., 2020; Sauerbeck et al., 2018). Astrocyte activation has primarily been observed only in major white matter tracts (CC and OPT) after CHIMERA, but in CCI and FPI astrocytes can be seen forming a glial scar around the area of the lesion (Osier et al., 2015). Histopathology after CHIMERA more closely resembles other closed-skull TBI models such as the weight drop model in producing diffuse axonal damage without the type of cell death produced in CCI or FPI (Osier et al., 2015). Bodnar et al. (2019) provide a thorough summary comparing results from different methods of closed-skull TBI, including CHIMERA.

In summary, injury produced by CHIMERA results in reliable pathological changes observed particularly in white matter and specifically in white matter integrity and inflammation, but the time course of these changes is variable. As the majority of studies reviewed used young, male C57BL/6 mice, additional research is recommended on how these pathological changes may differ in younger and older animals, females, and in other species. Finally, most studies used similar parameters, but because changing the direction of acceleration and rotation can also alter behavioral and molecular outcomes (Mychasiuk et al., 2016), further study of these alterations in the CHIMERA and how they affect pathology is suggested.

4.5. Imaging

Noninvasive, *in vivo* imaging is an important tool for clinical diagnosis of TBI. Magnetic resonance imaging (MRI) in the clinical setting, however, is primarily reserved for cases of moderate or severe TBI (Hernandez et al., 2016; Pautler, 2004). The majority of cases are mTBI; clinically defined as not having detectable computerized tomography (CT) imaging changes. The lack of sensitivity of traditional methods of CT and MRI may contribute to the underdiagnosis of mTBI (Hernandez et al., 2016; Kikinis et al., 2017). Pre-clinical experiments that incorporate imaging often display a correlation between imaging and pathological data. Many advances have been made to improve neuroimaging techniques for TBI, but imaging data alone cannot provide information about the mechanism of injury (Haber et al., 2017; Hutchinson et al., 2018; Komlosh et al., 2018).

Diffusion magnetic resonance imaging (dMRI) is favorable for mTBI

because of its sensitivity to detecting microstructural changes in water diffusion within tissue (Hutchinson et al., 2018; Kikinis et al., 2017). A common approach for dMRI is utilizing *ex vivo* brain tissue for imaging, which is unrestrained by time limitations and can allow for higher resolution images compared to *in vivo* scanning (Kikinis et al., 2017). dMRI has utility for detecting changes in axonal geometry, which can manifest as axonal varicosities and retraction bulbs causing a decrease in diffusivity (Budde et al., 2009; Hutchinson et al., 2018; Mac Donald et al., 2007). Previous studies with rotational acceleration TBI models have used *ex vivo* dMRI to show both variability in fractional anisotropy (FA) values for white matter regions and tracts (Stemper et al., 2015; Kikinis et al., 2017). FA values are typically reduced in damaged white matter tracts, but differences in biological mechanisms of injury and variations in scanning parameters could contribute to the mixture of dMRI outcomes (Hutchinson et al., 2018). In other commonly used models of TBI, such as CCI, FPI and weight drop, contusions and edemas are typically observed in T2-weighted MRI (Gold et al., 2013; Hutchinson et al., 2018). More diffuse trauma, such as blast TBI, demonstrated decreased FA values in white matter tracts and the cerebellum using DTI (Skotak et al., 2019). Additional imaging pathologies characteristic of TBI that have been reported include focal lesions and diffuse axonal injury (Gold et al., 2013). Neuroimaging after TBI, however, often displays mixed etiology with increased or decreased diffusivity or anisotropy depending on the injury severity and underlying cellular mechanisms (Hutchinson et al., 2018).

Since CHIMERA mainly induces white matter injury, dMRI was preferred because it detects CHIMERA's subtle white matter damage (Haber et al., 2017; Komlosh et al., 2018). Three out of the four CHIMERA neuroimaging papers utilized dMRI (Table 4), while the fourth, Nolan and colleagues, implemented T2-weighted MRI alone (Haber et al., 2017; Komlosh et al., 2018; Nolan et al., 2018; Sauerbeck et al., 2018). Both the Haber and Komlosh groups performed *ex vivo* dMRI in male C57BL/6 mice at about 7 days after the final CHIMERA injury. Sauerbeck and others also implemented *ex vivo* dMRI, but 2 days after modCHIMERA and with both male and female C57BL/6 mice. Despite different injury models, both Haber (2 × 0.5 J or 0.65 J, 24-h interval) and Sauerbeck (modCHIMERA: 1 × 1.7 J or 2.1 J) groups used more traditional DTI parameters. Komlosh and colleagues (3 × 0.5J, 24-h interval) implemented an advanced double pulse-field gradient (dPFG) sequence for increased sensitivity and specificity to cellular changes (Haber et al., 2017; Hutchinson et al., 2018; Komlosh et al., 2018; Sauerbeck et al., 2018). Nolan and colleagues (5 × 0.5 J, 24-h interval) conducted *in vivo* T2-weighted MRI in male C57BL/6 mice, but scanning took place about 40 days after impact (Nolan et al., 2018).

Subtle changes were observed in the DTI data, but not in the T2-weighted images alone (Haber et al., 2017; Komlosh et al., 2018; Nolan et al., 2018; Sauerbeck et al., 2018). Primary regions of interest in all four papers included white matter tracts, such as the corpus callosum (Haber et al., 2017; Nolan et al., 2018; Sauerbeck et al., 2018), optic tracts (Haber et al., 2017; Komlosh et al., 2018), and anterior commissure (Sauerbeck et al., 2018). After multiple comparison corrections, DTI showed significant changes in the brachium of the superior colliculus, optic tract, and hippocampus for various FA, diffusivity, and anisotropy metrics. Reduced FA values were revealed in the same regions, as well as in the corpus callosum and anterior commissure (Haber et al., 2017; Sauerbeck et al., 2018). The optic tract displayed reduced values in most of the DTI metrics for FA, radial and axial diffusivity, and planar and linear anisotropy, but still did not show changes for the T2-weighted images (Haber et al., 2017). The optic tract was also a key focus for Komlosh and colleagues. Although there was a small sample size, differences in the optic tracts between CHIMERA and sham animals were observed. Optic tract FA values for the CHIMERA mouse showed a reduction in the right optic tract compared to the sham. The dPFG sequence also showed lower values for the optic tracts suggesting axonal damage. Komlosh and colleagues also discovered asymmetrical values in the left and right optic tracts, which can be common in diffuse

axonal injury (Komlosh et al., 2018). White matter tracts, particularly the optic tract, appears to be a key area of investigation for CHIMERA and is ideal to study with dMRI because of its high coherence and simple geometry (Haber et al., 2017; Komlosh et al., 2018).

5. Neurophysiology

Little is known about other physiological aspects with CHIMERA, such as electrophysiological responses (Table 5). Differences in electroencephalography (EEG) power frequency bands have been reported following FPI, weight drop, and blast TBI models (Hajiaghamemar et al., 2019). In traditional TBI models, EEG recordings have also demonstrated overall hyperexcitability after TBI, particularly in the hippocampus, and reduced seizure threshold with severely injured FPI rodents developing seizures (Schmitt and Dichter, 2015). To date, no EEG studies have been performed following CHIMERA injuries, but network properties have begun to be explored with neurophysiological experiment. Nolan and colleagues performed whole cell voltage clamp studies 30–60 days post-injury in mice, in which they measured intrinsic excitability of layer V pyramidal neurons of the medial prefrontal cortex after injury and reported minimal changes, suggesting that overall neuronal excitability was not altered following CHIMERA (Nolan et al., 2018). In a follow-up study, Krukowski and colleagues performed a closer evaluation of excitatory synaptic input in the same region with a focus on neuronal subtypes; type A neurons projecting subcortically and type B neurons projecting via the corpus callosum to other cortical areas. It was found that type A neurons showed an increase in the frequency of spontaneous excitatory postsynaptic currents (sEPSC) after repetitive CHIMERA, but no change in amplitude, while type B neurons did not undergo any changes. The increase in sEPSC frequency suggests that type A neurons involved in risk-taking behavior are more active post-injury, but the lack of amplitude change could indicate an absence of change in synaptic inputs (Krukowski et al., 2020; Nolan et al., 2018).

Following a single CHIMERA impact at a higher impact level (2.5 J) with the PLA interface in mice, Bashir and colleagues performed *ex vivo* CA1 (*stratum radiatum*) hippocampal field recordings both 6 h and 14 days post-injury to determine possible mechanisms of impaired learning and memory following CHIMERA (Bashir et al., 2020). Decreased event amplitudes in injured mice were measured at both time points; the change at the acute time point reduction was associated with a reduction in vesicular glutamatergic transporter 1, a marker of presynaptic hippocampal glutamatergic vesicles. Although this may be one mechanism for the decreased event amplitudes, more investigation is needed to determine other possible mechanisms (Bashir et al., 2020).

Desai and colleagues sought to assess visual deficits following single and multiple CHIMERA injuries in mice (Desai et al., 2020). Visual evoked potentials were measured 35 days after CHIMERA *in vivo* with bright flashes of light and a recording electrode placed on the surface of the skull above the visual cortex. Mice that received multiple CHIMERA hits (3 × 0.55 J, 24-h interval) displayed significantly lower N1 amplitude values compared to single injury and sham animals. Reduced N1 amplitudes were observed after a single CHIMERA compared to shams, but a larger decrease occurred following multiple CHIMERA. The significant decrease in N1 amplitude demonstrates impairment in visual signaling for the multiple CHIMERA group. Electroretinography was also tested, but no impairment was found demonstrating that changes in visual evoked potentials were caused by trauma to the optic nerve or tract and not due to retinal impairment (Desai et al., 2020).

6. Behavioral effects

6.1. Righting reflex

The loss of righting reflex (LRR), or the amount of time it takes for an animal placed in a supine position to return to a prone position

Table 4
Neuroimaging changes after CHIMERA injuries.

Time following injury	Sample size	Parameters	Analysis (Regions of Interest, ROI)	Results	Injury parameters	Reference
40 days	n = 5–7 sham n = 5–7 CHIMERA	*In vivo* T2 MRI T2 parameters TE/TR = 11.6/2006 msec, echo train = 8, slice thickness = 0.5 mm, slice number = 20, number of averages = 2, matrix 256 × 256, field of view = 30 × 30 mm^2, scanning time = 2 min 12 sec	ROIs: CC, external capsule, CTX, HP, ventricles, total brain	No structural damage *In vivo* T2 MRI did not find any anatomical volumes or signals in CTX, HP, or white matter structures but found behavioral deficits	5 × 0.5 J, 24-h interval	Nolan et al. (2018)
Perfused 7 days after injury 9 days after perfusion *ex vivo* brain scanned	n = 5 sham n = 5 CHIMERA	*Ex vivo* DTI parameters 8 segments, TE and TR = 38/617 ms, 1 nex, 152 volumes, 100 μm resolution DWI parameter b = 250 and 500s/mm^2, 6 directions, 2 high b-value shells b = 1500–1700 and 3000–3800 s/mm^2, 32 directions T2 MSME same spatial dimensions as DWI, TE/TR = 30/3000 ms, nex = 1	ROIs based on silver stain: brachium of superior colliculus, cingulum bundle, CC, OPT Reference ROIs: external capsule, internal capsule, CTX, HP, thalamus 2 random forests analysis classifier algorithm: DTI metric and ROI combination as a feature	T2 images showed no changes Decreased FA in OPT, brachium of superior colliculus, anterior CC, cingulum bundle, a bit in HP Top 3 ROIs for DTI random forests analysis were left and right OPTs and right HP Top 3 ROI for histology random forests analysis were left and right brachium of the superior colliculus and left OPT Location of changes in DTI and histology matched	2 × 0.5 J or 0.65 J, 24-h interval	Haber et al. (2017)
Perfused 7 days after last injury	n = 1 sham n = 1 CHIMERA	*Ex vivo* DTI MRI parameters: TE/TR = 23/700 ms, 8 segments, voxel resolution 100 × 100 × 100 μm^3 DTI parameters: δ = 3ms, Δ = 20ms, b-value 400 and 2000s mm-1 dPFG parameters same as DTI, but τm = 0, δ = 3 ms, Δ = 20 ms T2 weighted images parameters TE/TR = 40/2000 ms, voxel resolution 100 × 100 × 100 μm^3	Left and right OPT ROIs were manually drawn	OPT FA values for CHIMERA was 0.66 and 0.75, FA for Sham was 0.79 and 0.78 Axon mean diameter values from dPFG showed OPT sham 4.8 μm and 5.2 μm, and 8.6 μm and 5.4 μ for CHIMERA Axonal varicosities were observed in NF light chain staining in CHIMERA OPT	3 × 0.5 J, 24-h interval	Komlosh et al. (2018)
Perfused 2 days after last injury	n = 4 sham n = 6 modCHIMERA	*Ex vivo* DTI DTI parameter: TE/TR = 36 ms/1.5 sec, b = 0 and 2000s/mm^2, 15 directions, matrix 128 × 128, field of view = 15 × 15 mm^2, in-plane resolution 117 × 117 μm, slice number = 12, slice thickness = 0.5 mm	ROIs: CC, anterior commissure, HP commissure, fimbria	modCHIMERA at 1.7 J showed reduced FA in anterior commissure and CC	modCHIMERA, 1 × 1.7 or 2.1 J	Sauerbeck et al. (2018)

Abbreviations. CC: corpus callosum; CTX: cortex; dPFG: double pulsed-field gradient; DTI: diffusion tensor imaging; FA: fractional anisotropy; HP: hippocampus; OPT: optic tract; NF: neurofilament; TE/TR: echo time/repetition time; MSME: multiscale multiecho; DWI: diffusion weighted imaging; δ: gradient pulse duration; Δ: diffusion time; τm: water time constant

Table 5
Neurophysiology changes after CHIMERA injuries.

Time following injury	Animal details	Sample size	Reference (stimulation) electrode	Recording electrode	Results	Injury parameters	Reference
36–51 days	Male C57BL/6, 8 weeks old at time of injury	n = 4 mice per injury condition 3–4 cells per animal	n/a	*Ex vivo* whole cell recording, Layer V pyramidal neurons in medial prefrontal cortex	No changes in intrinsic excitability following injury	5 × 0.5 J, 24 h interval	Nolan et al. (2018)
35–60 days	Male and female C57BL/6J 8–10 weeks old	Type A (n = 11 sham, 7 CHIMERA rTBI, 9 CHIMERA rTBI + injection) Type B (n = 7 sham, 5 CHIMERA rTBI, 8 CHIMERA rTBI + injection) 1–4 neurons recorded per animal	n/a	*Ex vivo* whole cell recording Layer V pyramidal neurons in medial prefrontal cortex	No changes in intrinsic excitability or amplitude After CHIMERA rTBI, Type A (subcortical) neurons increased sEPSC frequency No change in Type B (callosal) neurons	5 × 0.5 J, 24 h interval	Krukowski et al. (2020)
35 days	C57BL/6NCr 4-5 months old	n = 10 mice	Lower lip	*In vivo* skull over the visual cortex	Significantly reduced N1 amplitudes following repeated, but not single CHIMERA N1 amplitude recording: sham was 59.3 +/- 4.03 single TBI 41.6 +/- 5.3 multiple TBI 16 +/- 3.6	1 × or 3 × 0.55 J, 24 h interval	Desai et al. (2020)
6 h and 14 days	Male and female C57BL6 5–7 months old	n = 3–4 mice per injury condition Brain slices: n = 24 sham, 16 6 h TBI, 12 14 day TBI	Schaffer collaterals (stimulating)	*Ex vivo* CA1 *stratum radiatum*	Decreased hippocampal event amplitudes after both 6 h and 14 days	1 × 2.5 J with PLA interface	Bashir et al. (2020)

Abbreviations. sEPSC: spontaneous excitatory postsynaptic currents; PLA: polylactic acid; rTBI: repetitive TBI

Table 6
Behavioral changes after CHIMERA injuries.

General behavior domain	Specific test	Animal details	Injury parameters	Testing time following injury	Results	Reference(s)
Motor	Rotarod	Male C57BL/6, ~4 months old at time of injury	2 × 0.5 J, 24-h interval	Up to 14 days	CHIMERA induces motor deficits for approximately 1 week	Namjoshi et al. (2014, 2016)
		C57BL/6-C3H, ~5.7 - 13.5 months old at time of injury	2 × 0.5 J, 24-h interval	From Day 1, up to 8 months	No effect of injury	Cheng et al. (2018, 2019)
		Male C57BL/6, 4 months old at time of injury	1 × 0.1–0.7 J	Up to 14 days	Motor deficits up to 14 days after 0.6–0.7 J	Namjoshi et al. (2017)
		Male and female C57BL/6J mice, 16 weeks old at time of injury	modCHIMERA, 1 × 1.7 J or 2.1 J	Days 1, 3, 7	No effect of injury	Sauerbeck et al. (2018)
	Beam-walk	Male C57BL/6 mice (Charles River), 12 weeks old	3 × 0.6 J, 24-h intervals	Days 1, 3, 5	Motor deficits 1 and 3 days post-injury	Chen et al. (2017)
	Open field	Male C57BL/6, 4 months old at time of injury	2 × 0.5 J, 24-h interval	Days 1, 7, 14	No effect of injury on distance traveled or immobility	Namjoshi et al. (2014)
		C57BL/6-C3H, 6.1 or 13.5 months old at time of injury	2 × 0.5 J, 24-h interval	Days 1 and 6	No effect of injury on distance traveled or immobility	Cheng et al. (2018)
		Male C57BL/6 mice 4–5 months old at time of injury	1 × 0.55 J or 5 × 0.55 J	Day 32	Increased distance traveled after repeated, but not single injury	Desai et al. (2020)
Cognition	Barnes maze (spatial learning and memory)	Male C57BL/6, 4 months old at time of injury	2 × 0.5 J, 24-h interval	Days 9–13	Main effect of injury on latency to locate escape tunnel (impaired memory)	Namjoshi et al. (2014)
		Male C57BL/6 mice, 5–7 months old at time of injury	PLA interface, 1 × 2.5 J	2 weeks to a month, or 2 months	No effect of injury on latency to locate escape tunnel during standard or reversal trials. Injured mice were impaired on probe trials at 2 weeks/month time point	Bashir et al. (2020)
		C57BL/6-C3H, 6.1 or 13.5 months old at time of injury	2 × 0.5 J, 24-h interval	Days 8–12	No deficits in the injured younger mice; older injured mice had impaired memory on one testing day (Day 9)	Cheng et al. (2018)
		C57BL/6-C3H, 5.7 months old at time of injury	2 × 0.5 J, 24-h interval	Days 14–18, probe trials Days 19, 2 months, 6 months, 8 months. Reversal trials on the day following each probe trial.	Injured mice impaired on days 14, 15, 17 with the use of less efficient search strategies. No effects of injury on probe or reversal trials.	Cheng et al. (2019)
	Modified Barnes maze (working memory)	Male C57BL/6J mice, 8 weeks old at time of injury	0.5 J × 5, 24-h intervals	Days 32–35	Injured mice impaired on days 33–35; did not show significant within-day learning until day 35 (compared to shams on day 33)	Nolan et al. (2018)
	Morris water maze	Male C57BL/6 mice (Charles River), 12 weeks old	3 × 0.6 J, 24-h intervals	1 and 6 months	Latencies (but not distances) to platform were longer in injured mice on 2 days at 1 month, and 1 day at 6 months. Injured mice impaired on probe trial at both time points. No effect on swim speed.	Chen et al. (2017)
		Male hTau mice, 4 months old at time of injury	20 × 0.13 J or 0.24 J, 24-h intervals	1, 3 and 12 months	Decreased swim speeds in injured mice. Distances to platform longer during visible and hidden training trials at all time points. Injured mice impaired on probe trial at all time points.	Gangolli et al. (2019)
		Male and female C57BL/6J mice, 16 weeks old at time of injury	modCHIMERA, 1 × 1.7 J or 2.1 J	3 weeks	Both injury levels resulted in greater distances to the platform and impairments on the probe trial. No effect on swim speed.	Sauerbeck et al. (2018)
	Passive avoidance (working memory)	Male C57BL/6, 4 months old at time of injury	2 × 0.5 J, 24-h interval	Days 7–10	Effect of injury on latency to enter darkened compartment on all days (impaired memory)	Namjoshi et al. (2014)
		C57BL/6-C3H, ~5.7 - 13.5 months old at time of injury	2 × 0.5 J, 24-h interval	From Day 1, multiple testing time points up to 8 months	No effect of injury	Cheng et al. (2018, 2019)
		APP/PS1 mice	2 × 0.5 J, 24-h interval	Day 6 and 6 months	Enhanced fear response after injury	Cheng et al. (2019)
Impulsivity	Delay discounting task	Male Long-Evans rats, 4.5 months at time of injury	1 × 2.9 J, 4 × 2.4 J, 2-week intervals	Testing performed in intervals between injuries and following final injury	Injured rats showed greater impulsivity	Vonder Haar et al. (2019)
Aggression	Resident intruder test	Male C57BL/6, 15 weeks old at time of injury	2 × 0.5 J, 24-h interval	Day 5	No effect of injury	Namjoshi et al. (2016)

Table 6 (*continued*)

General behavior domain	Specific test	Animal details	Injury parameters	Testing time following injury	Results	Reference(s)
Anxiety	Open field	Male C57BL/6, 4 months old at time of injury	2 × 0.5 J, 24-h interval	Days 1, 7, 14	Increased thigmotaxis for two weeks following injuries	Namjoshi et al. (2014)
		Male C57BL/6, 4 months old at time of injury	1 × 0.1–0.7 J	Days 1 and 7	Increased thigmotaxis at Days 1 and 7 after 0.6–0.7 J	Namjoshi et al. (2017)
		Male and female C57BL/6J mice, 16 weeks old at time of injury	modCHIMERA, 1 × 1.7 J or 2.1 J	Days 1 and 7	Increased thigmotaxis after 1.7 and 2.1 J on Day 1	Sauerbeck et al. (2018)
		Male C57BL/6 mice 4–5 months old at time of injury	1 × 0.55 J or 5 × 0.55 J	Day 32	Increased thigmotaxia after repeated, but not single injury	Desai et al. (2020)
	Elevated plus maze	Male C57BL/6 mice, 4–5 months old at time of injury	1 × 0.1–0.7 J	Day 2	No effect of injury	Namjoshi et al. (2017)
		C57BL/6-C3H, 6.1 or 13.5 months old at time of injury	2 × 0.5 J, 24-h interval	Days 7 and 11	No effect of injury	Cheng et al. (2018)
		C57BL/6-C3H, 5.7 months old at time of injury		Days 7 and 10; 1, 2, 3, 6, 7 and 8 months	Main effect of injury; CHIMERA increased time spent in open arms	Cheng et al. (2019)
		Male C57BL/6J mice, 8 weeks old at time of injury	5 × 0.5 J, 24-h intervals	Day 26	CHIMERA increased time spent in open arms	Nolan et al. (2018)
		Male and female C57Bl/6J mice, 8–10 weeks old at time of injury	5 × 0.5 J, 24 h intervals	1 month	CHIMERA increased time spent in open arms in male mice only	Krukowski et al. (2020)
		Male and female C57BL/6J mice, 16 weeks old at time of injury	modCHIMERA, 1 × 1.7 J or 2.1 J	Day 26	No significant effects, strong trend toward increased open arm time in injured male mice	Sauerbeck et al. (2018)
		Male hTau mice, 4 months old at time of injury	20 × 0.13 J or 0.24 J, 24-h intervals	Day 26, 3 months and 1 year	No effect of injury	Gangolli et al. (2019)
Depression	Tail suspension test	Male and female C57BL/6J mice, 16 weeks old at time of injury	modCHIMERA, 1 × 1.7 J or 2.1 J	1 month	No effect of injury	Sauerbeck et al. (2018)
		Male hTau mice, 4 months old at time of injury	20 × 0.13 J or 0.24 J, 24-h intervals	Day 40, 3 months and 1 year	Decreased immobility after 0.24 J × 20	Gangolli et al. (2019)
	Forced swim test	Male C57BL/6 mice, 5–7 months old at time of injury	PLA interface, 1 × 2.5 J	Day 45	No effect of injury	Bashir et al. (2020)
Social interaction	Sociability test	Male and female C57BL/6J mice, 16 weeks old at time of injury	modCHIMERA, 1 × 1.7 J or 2.1 J	Day 27	Deficits in social interaction, but not social novelty after 2.1 J	Sauerbeck et al. (2018)
		Male C57BL/6J mice, 8 weeks old at time of injury	5 × 0.5 J, 24-h intervals	Days 27–28	Deficits in social novelty, but not social interaction following CHIMERA	Nolan et al. (2018)
		Male hTau mice, 4 months old at time of injury	20 × 0.13 J or 0.24 J, 24-h intervals	3 weeks, 3 months and 1 year	No effect of injury	Gangolli et al. (2019)

following injury, is often employed in pre-clinical TBI studies as a measure of loss of consciousness (e.g., (Velosky et al., 2017; Yu et al., 2017)). Namjoshi and colleagues found that LRR was one of the most sensitive measures for discriminating C57BL/6 mice that had sustained sub-threshold (0.1, 0.2, 0.3, or 0.4 J), threshold (0.5 J) or mild TBI (0.6–0.7 J) levels of impact by CHIMERA (Namjoshi et al., 2017). Specifically, sub-threshold CHIMERA resulted in LRR durations equivalent to those of sham controls (approximately 1 min), whereas threshold and mild TBI had longer LRR durations of approximately 3 and 6 min, respectively. Using a finer range of impact pressures between zero and 2.4 psi (0.4 J), Gangolli and colleagues reported that a minimum energy level of approximately 0.13 J is necessary to increase the LRR above the duration of sham controls (approximately 1 min) and determined this energy level to be sub-threshold. This sub-threshold level is substantially lower than the sub-threshold level of 0.4 J and below defined by previous work (Namjoshi et al., 2017), and the authors noted that the findings are inconsistent (Gangolli et al., 2019). Furthermore, when mice sustained 20 sub-threshold injuries (daily), the average righting reflex time was not significantly different from that of sham-treated animals.

Application of the modCHIMERA version, which used higher energy levels (1.7 J and 2.1 J) in helmeted mice, increased the duration of the LRR in a dose-dependent level (Sauerbeck et al., 2018) and the LRR was noticeably longer than for traditional CHIMERA: approximately 9 min at 1.7 J and approximately 18 min at 2.1 J. Bashir and colleagues also used a higher impact energy (2.5 J) in mice with a PLA interface to distribute energy, and found that the LRR was greater than 30 min following a single impact (Bashir et al., 2020). The LRR has also been reported in rats that have sustained 5 × CHIMERA (first impact 2.9 J, subsequent impacts 2.4 J, with 14 days between injuries) (Vonder Haar et al., 2019). Although brain injury increased the LRR compared to sham controls (approximately 4 min), the effect did not reach statistical significance.

6.2. Sensory systems

To date, Desai and colleagues are the only investigators to explore potential sensory deficits; they employed multiple measures to assess potential visual dysfunction following single and repeated CHIMERA (Desai et al., 2020). Visible platform trials are often conducted in the Morris water maze (MWM) either prior to or subsequent to hidden platform trials to ensure the animals have proper visual function and can employ the visual cues to properly perform the task (Tucker et al., 2018). Desai and colleagues performed 3 days of visible platform acquisition trials 19 days following injuries, and demonstrated that mice that sustained multiple (3 × 0.55 J, 24-h intervals), but not single (0.55 J), CHIMERA impacts were significantly impaired during these trials; they had significantly longer latencies and distances swam to reach the visible platform (Desai et al., 2020). These deficits were accompanied by optic tract astrogliosis, impairments on the visual cliff behavioral test of visual acuity, as well as significantly deviated visual evoked potentials 5 weeks after injuries (see Neurophysiology section for details) (Desai et al., 2020). Taken together, these results suggest that multiple injuries with CHIMERA may lead to visual deficits. Further, they emphasize the need to consider potential sensory and/or motor deficits when selecting behavioral tests to avoid confounds.

6.3. Motor behaviors

Motor skills have been reliably impaired in mice following CHIMERA brain injury, assessed primarily by the rotarod test and beam walking (Table 6). Namjoshi and colleagues initially demonstrated that CHIMERA (2 × 0.5 J, 24-h interval) induces motor deficits, as assessed by latency to fall from an accelerating rotarod, for approximately 1 week following injuries in male C57BL/6 mice (Namjoshi et al., 2016; Namjoshi et al., 2014). Subsequent studies did not find rotarod deficits

following CHIMERA with equal injury parameters (Cheng et al., 2019; Cheng et al., 2018), but the mice employed in those experiments were older (~5.7–13.5 months old), hybrid C57BL/6-C3H mice and the authors suggested the genetic background may have provided resilience to the behavioral effects of mild TBI.

In a later study intended to define the threshold for biological and functional effects of the injury, it was reported that an energy level of 0.6 J – 0.7 J was classified as "mild TBI," and this was the minimum injury level required with a single impact to result in rotarod deficits (Namjoshi et al., 2017). Different parameters of CHIMERA have been explored by other laboratories; Chen and colleagues repeated the CHIMERA impact (3 × 0.6 J, 24-h intervals) and reported impairments on a beam-walk task at one and three, but not 5, days following injuries (Chen et al., 2017). No motor impairment on the rotarod was found following modCHIMERA (1.7 J or 2.1 J) (Sauerbeck et al., 2018).

General ambulation and exploration can be measured in an open field (OF) environment. Desai and colleagues reported hyperactivity (increased total distance traveled) in the OF following repeated (3 × 0.55 J, 24-h interval), but not single (0.55 J) CHIMERA hits (Desai et al., 2020). Hyperactivity is consistent with findings from other rodent TBI models such as CCI (e.g., (Tucker et al., 2017; Wakade et al., 2010; Yu et al., 2012) or repeated concussive brain injury (rCBI) (Kane et al., 2012; Mannix et al., 2014; Tucker et al., 2019). Over a period of 14 days post-injury, no changes in distance traveled or time spent immobile were observed following 2 × 0.5 J CHIMERA (Namjoshi et al., 2014). Cheng and colleagues also found in the hybrid C57BL/6-C3H mouse that there were no effects of CHIMERA (2 × 0.5 J) on immobility or distance traveled on days one or six following injury (Cheng et al., 2018). These results suggest repeated and/or higher energy CHIMERA impacts may induce hyperactivity; also, that motor impairments following CHIMERA injury are limited to more sensitive and challenging tasks, such as the rotarod and beam walk, and more general ambulatory locomotion is unimpaired (Table 6). However, there is a large range of available tasks spanning vestibulomotor, sensorimotor, strength and reflexes, gait tests, and other fine motor skills (e.g., grid walk and adhesive removal test) (Fujimoto et al., 2004), on which function following CHIMERA injury remains unexplored.

6.4. Cognition

Cognition (e.g., learning and memory) is likely the most widely-tested behavioral domain following experimental TBI, and the MWM is the most popular test due to its robustness in detecting the effects of mild to severe TBI and flexibility in testing paradigms (Tucker et al., 2018). The MWM has been well-employed following CHIMERA injury (Chen et al., 2017; Gangolli et al., 2019; Sauerbeck et al., 2018), as has the similar, dry-land version, the Barnes maze (Bashir et al., 2020; Cheng et al., 2019; Cheng et al., 2018; Namjoshi et al., 2014; Nolan et al., 2018), both of which test spatial learning and memory (Table 6). These hippocampal-dependent tests require the animal to use distant, spatial cues to navigate an aversive environment to learn the location of an escape platform (MWM) or darkened tunnel beneath the arena (Barnes maze). Employing the Barnes maze in the first CHIMERA report, Namjoshi and colleagues demonstrated significant main effects of injury in the primary latency to locate the escape tunnel during learning trials nine to 13 days following injuries (2 × 0.5 J, 24-h interval) in C57BL/6 mice (Namjoshi et al., 2014). In hybrid C57BL/6-C3H mice tested with the same injury parameters at the same time following CHIMERA, no deficits were reported in the younger (~6.1 months old) mice, but latencies to find the tunnel were longer in the older (~13.5 months old) injured mice on one of the testing days (day 9) (Cheng et al., 2018). In slightly younger (~5.7 months old) hybrid C57BL/6-C3H mice, the same injury parameters (2 × 0.5 J, 24-h interval) resulted in impaired performance in injured mice on three training days (days 14, 15 and 17 following injuries). Further analysis of "search strategies" of the animals, in which an animal's movement path is

tracked and categorized according to path efficiency (Illouz et al., 2016), showed that CHIMERA-treated mice were more likely to use less-efficient search strategies in the maze (e.g., random paths) rather than taking more direct paths to the escape tunnel (Cheng et al., 2019). The mice were further tested up to 8 months post-injury on probe trials, in which the escape tunnel is removed from the maze and memory is assessed by measuring the amount of time spent near the previous target location. Reversal trials, in which the escape tunnel is placed in a new location to re-test learning and cognitive flexibility, were performed after probe trials. There were no effects of injury on the probe or reversal trials performed 2, 6 and 8 months after CHIMERA (Cheng et al., 2019).

The same group of investigators tested the effects of a single impact at a higher energy level (2.5 J) with the PLA interface on Barnes maze performance (Bashir et al., 2020). No effects of injury were reported on spatial learning (or reversal learning) in mice tested 2 weeks to a month following injury, or in a separate group of mice tested 2 months following injury. However, there was a significant effect of injury on probe trials performed on animals tested at the earlier time point, with injured mice spending less time near the target location, suggesting impaired memory (Bashir et al., 2020).

Nolan and colleagues employed a modified version of the Barnes maze in a delayed matching-to-sample task, intended to test working memory, in which the escape tunnel was relocated each day and the animals had to re-learn the new location (Nolan et al., 2018). Injured C57BL/6J mice (5 × 0.5 J, 24-h intervals) were significantly impaired in their ability to locate the escape tunnel on days 33–35 following injuries, compared to sham controls. As the mice are required to learn a new escape location each day, the authors also analyzed the learning that occurred within each day by comparing the first and last trials, and found that sham-treated mice showed significant learning on day 33, but injured mice did not have significant learning until day 35 (Nolan et al., 2018).

Spatial learning and memory deficits have also been reported following repeated CHIMERA impacts in mice assessed in the MWM (Chen et al., 2017; Gangolli et al., 2019; Sauerbeck et al., 2018). C57BL/6 mice had a longer latency to locate the hidden platform in the MWM approximately 1 month following repetitive (3 × 0.6 J, 24-h intervals) CHIMERA, on the third and fourth days of training (Chen et al., 2017). In a subsequent probe trial, the injured mice also spent significantly less time in the quadrant that formerly housed the escape platform. Slight differences between groups during training trials remained at the 6-month period following injuries, and injured mice were still significantly impaired on the probe trial at this time point (Chen et al., 2017).

Chen and colleagues reported no changes as a function of injury on swim speed in the MWM in wild-type mice, an important control measure particularly in TBI experiments in which motor deficits may be present, as differences between groups in swim speeds may confound latency measures (Tucker et al., 2018). However, hTau mice had significantly slower swim speeds in the MWM following repeated CHIMERA at either sub-concussive (20 × 0.13 J, 24-h intervals) or concussive (20 × 0.24 J, 24-h intervals) levels (Gangolli et al., 2019), and wild-type mice were shown to have slower swim speeds during visible platform trials following repeated (5 × .55 J, 24-h intervals) CHIMERA (Desai et al., 2020). Reporting path length or distance swam to the platform as the primary measure of learning during acquisition trials may partially control for differences in swim speed, and concussive levels of repeated CHIMERA resulted in significantly longer path lengths to the platform during visible and/or hidden training trials in the hTau (Gangolli et al., 2019) and wild-type (Desai et al., 2020) mice. The injured hTau mice also showed impaired memory during the probe trials at the acute and chronic time points, as evidenced by decreased time spent in the target quadrant and a greater mean distance from the former platform location. Deficits on the test were correlated with white matter integrity, specifically microgliosis (Gangolli et al., 2019).

Reduced swim speeds during the visible and hidden platform trials were associated with increased Iba1 staining in the corpus callosum and hippocampal commissure, whereas cognitive deficits during training and probe trials were positively correlated with microgliosis in the corpus callosum and fimbria (Gangolli et al., 2019). modCHIMERA, either 1.7 or 2.1 J, also resulted in learning and memory deficits in the MWM. Approximately 3 weeks following injury, there were no significant differences in swim speed between groups, but both injury levels resulted in greater distances swam to the platform during training trials, and greater mean distances from the previous location of the platform during the probe trial (Sauerbeck et al., 2018).

Another test employed to demonstrate cognitive deficits following CHIMERA-induced TBI is the passive avoidance (PA) task. Mice are trained on an initial day by placing them in a brightly-lit half of a two-chamber shuttlebox, and when they enter the darkened half a footshock is delivered. On subsequent days, animals are placed into the light portion of the box and the latency to enter the dark half is measured. Eight to 10 days following repeated CHIMERA (2 × 0.5 J, 24-h interval), injured C57BL/6 mice had shorter latencies to enter the darkened portion of the apparatus, indicating impaired working memory (Namjoshi et al., 2014). Repeated CHIMERA (2 × 0.5 J, 24-h interval) had no effect on working memory in the PA task in hybrid C57BL/6-C3H mice when tested at acute (1 week) or more chronic (1–3 months) time points (Cheng et al., 2019; Cheng et al., 2018). Interestingly, APP/PS1 mice that sustained TBI exhibited an enhanced fear responses on PA testing at early (6 days) and later (6 months) times after injury (Cheng et al., 2019).

6.5. Impulsivity

Vonder Haar and colleagues employed the delay discounting task (DDT) to assess changes in impulsive behaviors in rats as multiple CHIMERA impacts are delivered (Vonder Haar et al., 2019). The DDT assesses impulsivity by allowing a subject to choose an immediate, smaller reward, or a delayed, larger reward. As the delay to the larger reward increases, subjects will begin to choose the smaller reward. More "impulsive" subjects are intolerant of the increasing delay and will begin to choose the smaller reward sooner. Rats that had been previously trained and had reached a stable baseline on the DDT were given five impacts (first impact 2.9 J, subsequent impacts 2.4 J) at 2-week intervals, and during the intervals between impacts they were assessed on the DDT for changes in impulsive behaviors. Compared to sham-treated rats, injured animals were more impulsive on the DDT, particularly after the fourth and fifth impacts. Further analysis showed that, when compared to baseline testing, the performance of the injured mice began declining after the first CHIMERA impact and continued to deteriorate after each subsequent injury except the last (Table 6). Final performance on the DDT was significantly correlated with corpus callosum thickness and phosphorylated tau deposition in the optic tracts, with poorer performance associated with corpus callosum thinning and greater amounts of phosphorylated tau. However, behavioral deficits were not correlated with pathological changes in neural circuitry underlying DDT performance, the mesolimbic reward circuit (Vonder Haar et al., 2019).

6.6. Aggression

Despite aggression being a symptom associated with clinical presentation of repeated head injuries, particularly CTE (Mahar et al., 2017), there is a paucity of studies looking for signs of aggression in rodents following rCBIs. Namjoshi and colleagues employed the resident intruder test (Namjoshi et al., 2016), in which an "intruder" mouse is placed into the home cage of a singly-housed "resident" mouse, and the latency to the beginning of an aggressive interaction is recorded. Other threat behaviors such as mounting or tail rattling may also be quantified. Five days following repeated CHIMERA (2 × 0.5 J,

24-h interval), injured mice did not display increased aggressive interactions compared to sham controls (Table 6) (Namjoshi et al., 2016). Despite this negative finding, future translational studies on rCBIs and CHIMERA specifically should continue to explore aggression given its clinical relevance.

6.7. Anxiety

The OF arena allows a preliminary measure of anxiety by measurement of thigmotaxis, the amount of time the animal spends around the edges of the apparatus versus the center. Increased thigmotaxis, indicative of greater anxiety, has been reported about 1 month following repeated (2 × 0.55 J, 24-h intervals), but not single (0.55 J), CHIMERA (Desai et al., 2020), and for 2 weeks following repeated injuries (2 × 0.5 J, 24-h intervals) (Namjoshi et al., 2014). In a follow-up study of single-impact CHIMERA, it was found that a single impact at a "mild TBI" level (0.6–0.7 J), but not sub-threshold (0.1–0.4 J) or threshold (0.5 J) level, resulted in increased thigmotaxis in the OF for 1 week following injuries (Namjoshi et al., 2017). After modCHIMERA (both 1.7 J and 2.1 J), thigmotaxis was increased the day following injury, but returned to levels of sham controls within 1 week (Sauerbeck et al., 2018).

A more formal test for anxiety-like behaviors in rodents is the elevated-plus maze (EPM), in which an animal chooses to explore dark, enclosed arms or open, exposed arms arranged in a plus-shape and raised above the floor (Lister, 1987). Several CHIMERA studies have employed the EPM to assess anxiety. Namjoshi and colleagues found no changes in EPM behavior at an acute time point (2 days) following a single CHIMERA impact ranging from 0.1 to 0.7 J (Namjoshi et al., 2017). In hybrid C57BL/6-C3H mice, Cheng and colleagues also found no differences in EPM behavior following 2 × 0.5 J (24-h interval) CHIMERA when measured at relatively acute time points (days seven and 11 following injury) (Cheng et al., 2018), but when tested eight times over a period of 8 months following injuries, there was a main statistical effect of injury, where injured mice spent greater amounts of time in the open, exposed arms, suggesting reduced anxiety (Cheng et al., 2019). Increased open-arm time was also reported in wild-type male C57BL/6 mice about 1 month following 0.5 J × 5 (24-h interval) CHIMERA (Krukowski et al., 2020; Nolan et al., 2018), and although modCHIMERA did not result in a statistically-significant change in anxiety-like behaviors at the same time point, there was a strong trend toward increased open-arm time (Sauerbeck et al., 2018). In hTau mice with multiple sub-concussive (20 × 0.13 J, 24-h intervals) or concussive (20 × 0.24 J, 24-h intervals) impacts, there were no changes in EPM behavior 26 days, or three or 12 months following injuries (Gangolli et al., 2019).

In summary, the OF test has shown increased thigmotaxis, indicative of greater anxiety, in injured mice at more acute time periods (1–2 weeks) following multiple impacts or single injuries at higher energy levels. In contrast, results from the EPM indicate no changes in anxiety-like behaviors shortly following CHIMERA. At longer time points (several weeks after injury), however, some studies suggest decreased anxiety (greater time spent in open, exposed arms) which many investigators interpret as risk-taking behavior, or behavioral disinhibition, reported often in other mouse models of rCBI (Gold et al., 2018; Mannix et al., 2014; Mouzon et al., 2014; Petraglia et al., 2014; Tucker et al., 2019). Taken together these results may indicate a period of acute anxiety followed by long-term behavioral disinhibition (Table 6). Or, the differences may reflect the testing paradigm as conclusions regarding anxiety following experimental TBI have been shown to be test-specific (Popovitz et al., 2019; Tucker et al., 2017).

6.8. Depression

The tail suspension test (TST) is a common test for despair-like behavior, a symptom of depression, in which a mouse is suspended by

the tail and the amount of time the animal is in an immobile state is measured. Greater amounts of immobility indicate greater despair, and thus an increased state of depression (Malkesman et al., 2013; Steru et al., 1985). One month following modCHIMERA (1 × 1.7 or 2.1 J), there were no changes in duration of immobility in the TST (Sauerbeck et al., 2018). A lack of differences was also reported 45 days following a single CHIMERA with the PLA interface (1 × 2.5 J) in the forced swim test (FST), a similar test to the TST in which a mouse is placed in a cylinder of water and immobility is measured (Bashir et al., 2020). In the hTau mouse model that received 20 concussive impacts (0.24 J at 24-h intervals), however, immobility time in the TST was decreased compared to sham controls; this difference was most pronounced at the most acute time point tested (40 days following injury; Table 6) (Gangolli et al., 2019). This result suggests a decreased level of depressive-like symptomology, which is the opposite result expected based on clinical presentation of increased depressive symptoms following repetitive TBI. However, there have been other recent reports of decreased levels of immobility in the TST or the FST, following rCBIs in mice (Gold et al., 2018; Tucker et al., 2019). These results have been associated with a hyperactive phenotype (Tucker et al., 2019) and with increased time spent in bright and open regions in the EPM (Gold et al., 2018) or the related test, the EZM (Tucker et al., 2019). This group of symptoms could be related to TBI-related clinical presentations related to behavioral disinhibition, including impulsivity and risk-taking.

6.9. Social interaction

Symptoms related to social interaction are associated with depression as impairments in social function are prominent features of clinical depression (Kupferberg et al., 2016). A popular test for the study of social interaction in mice is the three-chambered sociability test, which allows the study of simple social interaction, social memory, and preference for social novelty (Moy et al., 2004). Deficits in social interaction, but not social novelty, were found 27 days following mod-CHIMERA at 1 × 2.1 J (but not 1 × 1.7 J) (Sauerbeck et al., 2018). After traditional repetitive CHIMERA (5 × 0.5 J, 24-h intervals, testing at 27–28 days) there were no differences between injured and sham-control mice in social interaction time (Nolan et al., 2018). The same negative results were reported in hTau mice when assessed 3 weeks, 3 months, and 1 year following sub-concussive (20 × 0.13 J, 24-h intervals) or concussive (20 × 0.24 J, 24-h intervals) CHIMERA (Gangolli et al., 2019). However, during the social novelty trial, injured wild-type mice spent significantly less time interacting with the "novel mouse," suggesting partial impairment in social memory (Nolan et al., 2018), perhaps related to working memory (Table 6). Social interaction has been shown to be impaired in a mouse model following repetitive mTBI (Yu et al., 2017), but some prior studies assessing sociability in mouse TBI models have found that TBI alone does not result in changes in social behaviors, but when TBI and stress are combined, social behaviors decrease (Klemenhagen et al., 2013; Mouzon et al., 2014). Future work will be needed to determine if sociability is affected by mild TBI alone.

6.10. Sex differences in behavior following CHIMERA

There has been very little study on sex differences in behavioral deficits following CHIMERA-induced injury. Krukowski and colleagues reported that the behavioral disinhibition observed in the EPM (increased time spent in the open arms) following repeated CHIMERA (5 × 0.5 J, 24-h intervals) was only seen in male, not female, mice (Krukowski et al., 2020). Sauerbeck and colleagues compared male and female mice on many behavioral tests following modCHIMERA at injury levels of 1.7 J and 2.1 J (Sauerbeck et al., 2018). They found similar nesting impairments in injured female and male mice, although uninjured female mice displayed poorer nesting behaviors compared to male mice. In the OF, injured female mice (2.1 J) were more active than

male mice (2.1 J) the day following injuries. Injured female mice (1.7 J) showed a slight advantage to injured male mice in the MWM, but injured females (2.1 J) had a reduction in social interaction behaviors compared to male mice (2.1 J). No sex differences were observed in the social novelty/memory test, rotarod, EPM, or TST (Sauerbeck et al., 2018).

6.11. Comparison to other TBI models

Despite being a relatively new TBI model, functional deficits following CHIMERA injury have been assessed on an impressively wide range of behavioral domains, particularly those most commonly studied following TBI: motor, cognitive, and neuropsychiatric symptoms. Motor and cognitive deficits like those shown following CHIMERA have been demonstrated for a couple of decades using classical TBI models such as CCI (e.g., (Fox et al., 1998; Leary et al., 2017; Tucker et al., 2016; Wagner et al., 2007)) and FPI (e.g., (Harrison et al., 2015; Huang et al., 2014; McIntosh et al., 1996; Saatman et al., 1996)), as well as with more recently-developed models including rCBI (e.g., (Jamnia et al., 2017; Tucker et al., 2019)) and blast injury (e.g., (Cernak et al., 2011; Yin et al., 2016)). However, results from neuropsychiatric symptom (i.e., anxiety, depression) testing have historically been less consistent (Malkesman et al., 2013; Tucker et al., 2017). For example, within the CCI model some investigators employing the EPM or EZM have reported increased anxiety (e.g., (Chauhan et al., 2010; Tchantchou et al., 2014)) while others have found reduced anxiety (e.g., (Tucker et al., 2017; Washington et al., 2012)) or no changes (e.g., (Amorós-Aguilar et al., 2015; Watanabe et al., 2013)), and the disparate results seem to not be explained by differences in injury location, severity, or time of testing after injury. Likewise, measured depressive symptoms in other TBI models have been variable; as described previously, reduced depressive symptoms have been reported following rCBI (Gold et al., 2018; Tucker et al., 2019), although others have found evidence of increased depression (e.g., (Klemenhagen et al., 2013; Petraglia et al., 2014)) or no changes (e.g., (Liu et al., 2017; Yang et al., 2015)). Comparatively, results to date from CHIMERA experiments have been quite consistent, with open field testing showing thigmotaxis (increased anxiety) at more acute (< 2 weeks post-injury) and EPM testing showing greater anxiety at later time points. In addition, results following tests of depressive-like symptoms are also relatively consistent, primarily with no changes found, or, decreased depressive symptomatology. This consistency compared to other experimental TBI models may be due to the standardized design and use of the device, and will expectantly continue to be borne out in future studies.

7. Summary and conclusions

7.1. Cumulative findings

The findings from the current CHIMERA literature can be summarized as follows. 1) The majority of CHIMERA studies thus far include a similar paradigm of 2 × 0.5 J injury separated by 24 h. 2) Pathological findings suggest that CHIMERA produces a diffuse injury with both acute and chronic damage in white matter tracts in particular. 3) Changes in microglial density and activation were observed after CHIMERA in white and grey matter. 4) Astrocyte activation was also found after injury. 5) Pathology, however, depends on the injury design and the time of analysis after impact. As found with other pre-clinical TBI models, for example, cytokine expression was acute and transient while the inflammatory response may not appear immediately following injury, but is potentially longer lasting. 6) Robust injury in white matter tracts, especially the optic tracts, following CHIMERA was demonstrated by histology and through DTI techniques. 7) The righting times and suggested loss of consciousness immediately subsequent to CHIMERA was found to display an increase in duration, as impact energy level was increased, but at least one group suggested this measure

is inconsistent. 8) Behavioral testing revealed consistent deficits in motor skills, such as beam walk and rotarod after CHIMERA injury, but no alteration in general ambulation. 9) The MWM and Barnes maze have been utilized in spatial learning and memory assessment with reported impairments post CHIMERA that are long lasting. 10) Compared to sham counterparts, injured rats displayed more impulsivity. 11) Results describing deficits in social interaction and social novelty are inconclusive and more data are needed. 12) Variability in anxiety-like behavior after CHIMERA may indicate an acute period of anxiety followed by long-term disinhibition. 13) Studies suggest CHIMERA injury does not induce depression symptoms. 14) A single study investigated potential sex differences in nesting behavior, motility, and social interaction and reported poorer nesting in uninjured females, more activity in injured females compared to injured males, and female social interaction impairment following CHIMERA.

7.2. CHIMERA challenges in application

CHIMERA, as a non-surgical procedure, allows study of the effects of "milder" repetitive injuries; the most frequently reported TBI malady. The development of a model that is available for commercial distribution allows for laboratories to employ the same devices, which lends to better opportunities for comparability. Likewise, CHIMERA devices for the mouse, rat, and ferret are similar in design, which offers the opportunity for simultaneous testing and comparison across commonly used species. However, dose-response studies for species, such as the experiment conducted by Namjoshi and colleagues in mice (Namjoshi et al., 2017), should be defined so that the CHIMERA can be scaled properly for differing animal models. The supplemental table provided by Namjoshi and colleagues, for example, provides a comparison for scaling of a few rotational models by reporting change in velocity, angular velocity, linear and angular acceleration, and Head Injury Criterion (Namjoshi et al., 2014). In addition to addressing potential scaling concerns between pre-clinical animal models, scaling to humans presents a challenge. As with other impact models, there is the need to balance the intensity of the injury within a range that results in tissue damage from acceleration, but minimizes compression injuries. Namjoshi and colleagues described a scaling process by using the equal stress/equal velocity as the basis for translatability to humans (Namjoshi et al., 2014; Viano et al., 2009). However, differences in anatomy may confound expectations, since sudden changes in velocity or rotation without linear motion lead to brain acceleration and deceleration with possible skull deformation. Rodents have more flexible bone structure than humans, which allows for reduced rates of velocity change and milder injury than can be sustained by the more rigid human skull (Cullen et al., 2016; Holbourn, 1943; Namjoshi et al., 2017; National Research Council Committee on Sports-Related Concussions in Youth, 2014; Ommaya et al., 1966). Given the limitation of many models to reduce compression injuries, such as skull fractures, the application must be performed with caution. One solution for CHIMERA and other closed-head injury studies requiring higher impact levels for higher acceleration has been the employment of a plate or helmet to dissipate the focal nature of impact force from the piston. However, a challenging limitation is careful standardization for the use of plate or helmet designs, which can vary between laboratories that employ them (cf., (McInnes et al., 2020)).

7.3. Maintenance for CHIMERA

Related to application, suggested maintenance is provided in the CHIMERA manual (University of British Columbia Wellington Laboratory and the Orthopedics and Injury Biomechanics Group, 2017). The piston barrel should be inspected regularly for abrasion or excessive wear, and cleaned of any debris that could alter piston function. The air compressor can be vulnerable to water and debris accumulation, which can be prevented by routine filter replacement. The

photogates are fragile and can affect the photocoupler velocity measurement if disturbed. Annual photogate validation with a high-speed video system is recommended to ensure accurate velocity reporting. If the velocity variation is greater than 4% at a set pressure, then recalibration and piston barrel cleaning are needed. Natural processes can affect machinery operation, such as rust formation, and regular inspection and care can determine the presence of loose components or screws. Complications can arise from misalignment of the piston barrel and photogate or body plate, piston rubber cap dislodgement, and software connection problems; thus requiring standard inspection.

7.4. Future prospects

The employment of CHIMERA as a model of impact-acceleration has the promise to broaden our understanding of the biological foundations of TBI. As with other pre-clinical models, there is a potential for confounding due to the use of anesthesia, and studies are needed that address the impact of anesthesia upon changes (Bodnar et al., 2019; Wojnarowicz et al., 2017). Since TBI often occurs in younger and older human populations, more research needs to be performed with male and female animals of various ages to enable further translatability (Faul et al., 2010). The majority of CHIMERA studies were performed in mice, with one study each in rats (Vonder Haar et al., 2019) and ferret (Whyte et al., 2019).

All CHIMERA reports (to date) have used the devices with animals in a supine position. This results in motion in the sagittal plane. In neonatal pigs, studies have indicated the sagittal plane results in greater injury, compared to horizontal or coronal rotation, for measures such as duration of consciousness and apnea, intracranial pressure, and degree of edema and intracranial bleeding (Cullen et al., 2016; Eucker et al., 2011), with horizontal rotation causing an intermediate level of pathology (Eucker et al., 2011; Sullivan et al., 2015). Earlier studies in primates observed that *coronal* rotation resulted in greater injuries than horizontal rotation (Gennarelli et al., 1982), and Maxwell and colleagues provided evidence that axons in the plane of a force (corpus callosum with coronal rotation in non-human primates) exhibit damage (Maxwell et al., 1993). Authors have speculated the disparities may result from species differences in the center of mass and center of rotation, and species differences in tract orientation related to how they are affected by the strain field (Cullen et al., 2016). Consistently, greater damage is sustained in tracts lying in the plane of rotation, and coronal rotation in the primate may essentially match horizontal plane effects in the pig as a result of cephalic flexure in primates (Cullen et al., 2016; Eucker et al., 2011). Reconfiguration of the CHIMERA devices allow a comparison of sagittal and horizontal impacts, and this will be of interest related to studies suggesting different planes of injury may result in varying functional and morphological outcomes (Browne et al., 2011; Mychasiuk et al., 2016).

Imaging studies with CHIMERA are to a certain extent limited to DTI, since CHIMERA shows subtle and diffuse injuries, which are difficult to detect. Only four articles with CHIMERA and neuroimaging have been published to our knowledge; thus, additional CHIMERA imaging is needed. The CHIMERA injury presents possible external damage from impact, but most of the pathology shows diffuse damage. The pathology included in the CHIMERA literature primarily focuses on microglial and astrocytic responses, but the staining pattern depends on the area of focus and time point after injury. Additional histological markers, such as further myelination change characterization, and time analyses with CHIMERA should be explored. As reviewed earlier, little is known about other physiological aspects with CHIMERA, such as electrophysiological and blood-brain barrier responses and a variety of behavioral tasks have yet to be tested after CHIMERA. Motor function has been evaluated with traditional methods, such as the rotarod and beam walk, but additional assessments for fine motor abilities have not been implemented. Only one study evaluated aggression, so another area for investigation includes aggression after repetitive CHIMERA

injuries. The potential effect of mTBI on sociability also has yet to be determined. The 19 CHIMERA publications have laid some groundwork for the emerging CHIMERA field, but the limited number of articles enables further investigation to confirm and extend upon the current findings.

7.5. Common data elements for CHIMERA

Detailed description of instrument application is a critical component of experiment reporting. It allows investigators to replicate conditions, make critical choices in their research planning, and evaluate the veracity of reported findings. Investigators of all publications reviewed here provided essential information regarding the unit of energy (Joule) that was applied (Table 1). However, the CHIMERA literature has not previously provided guidelines for what additional parameters should be reported. The need for model standardization has been recognized for decades (Margulies et al., 1990; Meaney et al., 1995), and common data elements were recognized in clinical research as an essential requirement for standardization (Hicks et al., 2013; Thurmond et al., 2010). Smith and colleagues recently outlined a comprehensive roster of common data elements (CDEs) for pre-clinical TBI studies that includes core CDEs that should be described in publications for all preclinical TBI models (Table 1 in (Smith et al., 2015)), as well as detailed identification of parameters specific to the most common pre-clinical TBI models (Tables 2–5 in (Smith et al., 2015)). These recommendations relate to comprehensive guidelines for experimental design considerations formulated by the National Institutes of Health (NIH) (https://www.nih.gov/research-training/rigor-reproducibility/principles-guidelines-reporting-preclinical-research), as well as an extensive list of CDEs (provided in ZIP files) on the Federal Interagency Traumatic Brain Injury Research website, https://fitbir.nih.gov/content/preclinical-common-data-elements#section-page-title. Akin to the report by Smith and colleagues, Table 7 provides suggested CDEs for investigators who employ the CHIMERA device. In addition to the core element reporting for animal phenotype, basic treatment variables and outcome measures (Table 1 in (Smith et al., 2015)), primary factors to consider are details regarding the model, data collection, and analysis description (Namjoshi et al., 2014; Smith et al., 2015).

Although there is some variablility in CHIMERA study designs, research standardization and proper machine maintenance will allow for valuable comparison and knowledge integration. The CHIMERA device enables reliable impact-rotational acceleration of animal models and consistent changes for behavior, imaging, and pathology have been reported. Findings thus far indicate motor and cognitive deficits and diffuse axonal injury following CHIMERA. The CHIMERA provides translatability opportunities for the clinically important mechanism of rotational acceleration.

Table 7
Closed-Head Impact Model of Engineered Rotational Acceleration (CHIMERA) relevant data elements.

Injury model characteristics	Air pressure (psi)-energy (Joules) calibration
Manufacturer	Change in velocity (m/s)
Impactor design (mass, material, shape, rigidity)	Linear velocity
Impactor retraction	Angular velocity (rad/s)
Storage tank pressure	Rotational velocity
Injury site (impact location)	Linear acceleration (g)
Angle of the animal on the platform	Angular acceleration (krad/s^2)
Modifications (helmet, body protection, animal stabilization method)	Rotational acceleration
Information regarding device calibration	Velocity of impactor (m/s)
Rotation range and plane	High speed camera analysis for head displacement

Declaration of competing interest

None of the listed authors have any personal, professional or financial conflicts of interest to declare.

Acknowledgements

References

Amorós-Aguilar, L., Portell-Cortés, I., Costa-Miserachs, D., Torras-Garcia, M., Coll-Andreu, M., 2015. Traumatic brain injury in late adolescent rats: effects on adulthood memory and anxiety. Behav. Neurosci. 129 (2), 149–159. https://doi.org/10.1037/bne0000046.

Armstrong, R.C., Mierzwa, A.J., Marion, C.M., Sullivan, G.M., 2016. White matter involvement after TBI: clues to axon and myelin repair capacity. Exp. Neurol. 275 (Pt 3), 328–333. https://doi.org/10.1016/j.expneurol.2015.02.011.

Bales, J.W., Wagner, A.K., Kline, A.E., Dixon, C.E., 2009. Persistent cognitive dysfunction after traumatic brain injury: a dopamine hypothesis. Neurosci. Biobehav. Rev. 33 (7), 981–1003. https://doi.org/10.1016/j.neubiorev.2009.03.011.

Bashir, A., Abebe, Z.A., McInnes, K.A., Button, E.B., Tatarnikov, I., Cheng, W.H., Haber, M., Wilkinson, A., Barron, C., Diaz-Arrastia, R., Stukas, S., Cripton, P.A., Wellington, C.L., 2020. Increased severity of the CHIMERA model induces acute vascular injury, sub-acute deficits in memory recall, and chronic white matter gliosis. Exp. Neurol. 324, 113116. https://doi.org/10.1016/j.expneurol.2019.113116.

Bodnar, C.N., Roberts, K.N., Higgins, E.K., Bachstetter, A.D., 2019. A systematic review of closed head injury models of mild traumatic brain injury in mice and rats. J. Neurotrauma 36 (11), 1683–1706. https://doi.org/10.1089/neu.2018.6127.

Browne, K.D., Chen, X.H., Meaney, D.F., Smith, D.H., 2011. Mild traumatic brain injury and diffuse axonal injury in swine. J. Neurotrauma 28 (9), 1747–1755. https://doi.org/10.1089/neu.2011.1913.

Budde, M.D., Xie, M., Cross, A.H., Song, S.-K., 2009. Axial diffusivity is the primary correlate of axonal injury in the experimental autoimmune encephalomyelitis spinal cord: a quantitative pixelwise analysis. J. Neurosci. 29 (9), 2805–2813. https://doi.org/10.1523/JNEUROSCI.4605-08.2009.

Cernak, I., Merkle, A.C., Koliatsos, V.E., Bilik, J.M., Luong, Q.T., Mahota, T.M., Xu, L., Slack, N., Windle, D., Ahmed, F.A., 2011. The pathobiology of blast injuries and blast-induced neurotrauma as identified using a new experimental model of injury in mice. Neurobiol. Dis. 41 (2), 538–551. https://doi.org/10.1016/j.nbd.2010.10.025.

Chauhan, N.B., Gatto, R., Chauhan, M.B., 2010. Neuroanatomical correlation of behavioral deficits in the CCI model of TBI. J. Neurosci. Methods 190 (1), 1–9. https://doi.org/10.1016/j.jneumeth.2010.04.004.

Chen, H., Desai, A., Kim, H.Y., 2017. Repetitive closed-head impact model of engineered rotational acceleration induces long-term cognitive impairments with persistent astrogliosis and microgliosis in mice. J. Neurotrauma 34 (14), 2291–2302. https://doi.org/10.1089/neu.2016.4870.

Cheng, W.H., Stukas, S., Martens, K.M., Namjoshi, D.R., Button, E.B., Wilkinson, A., Bashir, A., Robert, J., Cripton, P.A., Wellington, C.L., 2018. Age at injury and genotype modify acute inflammatory and neurofilament-light responses to mild CHIMERA traumatic brain injury in wild-type and APP/PS1 mice. Exp. Neurol. 301, 26–38. https://doi.org/10.1016/j.expneurol.2017.12.007.

Cheng, W.H., Martens, K.M., Bashir, A., Cheung, H., Stukas, S., Gibbs, E., Namjoshi, D.R., Button, E.B., Wilkinson, A., Barron, C.J., Cashman, N.R., Cripton, P.A., Wellington, C.L., 2019. CHIMERA repetitive mild traumatic brain injury induces chronic behavioural and neuropathological phenotypes in wild-type and APP/PS1 mice. Alzheimers Res. Ther. 11 (1), 6. https://doi.org/10.1186/s13195-018-0461-0.

Coronado, V.G., Haileyesus, T., Cheng, T.A., Bell, J.M., Haarbauer-Krupa, J., Lionbarger, M.R., Flores-Herrera, J., McGuire, L.C., Gilchrist, J., 2015. Trends in sports- and recreation-related traumatic brain injuries treated in US emergency departments: The National Electronic Injury Surveillance System-All Injury Program (NEISS-AIP) 2001-2012. J. Head Trauma Rehabil. 30 (3), 185–197. https://doi.org/10.1097/HTR.0000000000000156.

Corps, K.N., Roth, T.L., McGavern, D.B., 2015. Inflammation and neuroprotection in traumatic brain injury. JAMA Neurol. 72 (3), 355–362. https://doi.org/10.1001/jamaneurol.2014.3558.

Cullen, D.K., Harris, J.P., Browne, K.D., Wolf, J.A., Duda, J.E., Meaney, D.F., Margulies, S.S., Smith, D.H., 2016. A porcine model of traumatic brain injury via head rotational acceleration. Methods Mol. Biol. 1462, 289–324. https://doi.org/10.1007/978-1-4939-3816-2_17.

Defense and Veterans Brain Injury Center, 2019. DoD Worldwide Numbers for TBI Website. Date Accessed May 21, 2019. https://dvbic.dcoe.mil/dod-worldwide-numbers-tbi.

Desai, A., Chen, H., Kim, H.Y., 2020. Multiple mild traumatic brain injuries lead to visual dysfunction in a mouse model. J. Neurotrauma 37 (2), 286–294. https://doi.org/10.1089/neu.2019.6602.

Dixon, C.E., Lyeth, B.G., Povlishock, J.T., Findling, R.L., Hamm, R.J., Marmarou, A., Young, H.F., Hayes, R.L., 1987. A fluid percussion model of experimental brain injury in the rat. J. Neurosurg. 67 (1), 110–119. https://doi.org/10.3171/jns.1987.67.1.0110.

Eucker, S.A., Smith, C., Ralston, J., Friess, S.H., Margulies, S.S., 2011. Physiological and histopathological responses following closed rotational head injury depend on direction of head motion. Exp. Neurol. 227 (1), 79–88. https://doi.org/10.1016/j.expneurol.2010.09.015.

Faul, M., Wald, M.M., Xu, L., Coronado, V.G., 2010. Traumatic Brain Injury in the United States; Emergency Department Visits, Hospitalizations, and Deaths, 2002–2006 Website. Date Accessed May 21, 2019. https://www.cdc.gov/traumaticbraininjury/pdf/blue_book.pdf.

Fijalkowski, R.J., Stemper, B.D., Pintar, F.A., Yoganandan, N., Crowe, M.J., Gennarelli, T.A., 2007. New rat model for diffuse brain injury using coronal plane angular acceleration. J. Neurotrauma 24 (8), 1387–1398. https://doi.org/10.1089/neu.2007.0268.

Fleminger, S., Oliver, D.L., Lovestone, S., Rabe-Hesketh, S., Giora, A., 2003. Head injury as a risk factor for Alzheimer's disease: the evidence 10 years on; a partial replication. J. Neurol. Neurosurg. Psychiatry 74 (7), 857–862. https://doi.org/10.1136/jnnp.74.7.857.

Fox, G.B., Fan, L., Levasseur, R.A., Faden, A.I., 1998. Sustained sensory/motor and cognitive deficits with neuronal apoptosis following controlled cortical impact brain injury in the mouse. J. Neurotrauma 15 (8), 599–614. https://doi.org/10.1089/neu.1998.15.599.

Frugier, T., Morganti-Kossmann, M.C., O'Reilly, D., McLean, C.A., 2010. In situ detection of inflammatory mediators in post mortem human brain tissue after traumatic injury. J. Neurotrauma 27 (3), 497–507. https://doi.org/10.1089/neu.2009.1120.

Fujimoto, S.T., Longhi, L., Saatman, K.E., Conte, V., Stocchetti, N., McIntosh, T.K., 2004. Motor and cognitive function evaluation following experimental traumatic brain injury. Neurosci. Biobehav. Rev. 28 (4), 365–378. https://doi.org/10.1016/j.neubiorev.2004.06.002.

Gangolli, M., Benetatos, J., Esparza, T.J., Fountain, E.M., Seneviratne, S., Brody, D.L., 2019. Repetitive concussive and subconcussive injury in a human tau mouse model results in chronic cognitive dysfunction and disruption of white matter tracts, but not tau pathology. J. Neurotrauma 36 (5), 735–755. https://doi.org/10.1089/neu.2018.5700.

Gennarelli, T.A., 1994. Animate models of human head injury. J. Neurotrauma 11 (4), 357–368. https://doi.org/10.1089/neu.1994.11.357.

Gennarelli, T.A., Thibault, L.E., Adams, J.H., Graham, D.I., Thompson, C.J., Marcincin, R.P., 1982. Diffuse axonal injury and traumatic coma in the primate. Ann. Neurol. 12 (6), 564–574. https://doi.org/10.1002/ana.410120611.

Gold, E.M., Su, D., López-Velázquez, L., Haus, D.L., Perez, H., Lacuesta, G.A., Anderson, A.J., Cummings, B.J., 2013. Functional assessment of long-term deficits in rodent models of traumatic brain injury. Regen. Med. 8 (4), 483–516. https://doi.org/10.2217/rme.13.41.

Gold, E.M., Vasilevko, V., Hasselmann, J., Tiefenthaler, C., Hoa, D., Ranawaka, K., Cribbs, D.H., Cummings, B.J., 2018. Repeated mild closed head injuries induce long-term white matter pathology and neuronal loss that are correlated with behavioral deficits. ASN Neuro 10 https://doi.org/10.1177/1759091418781921. 1759091418781921.

Goldsmith, W., 2001. The state of head injury biomechanics: past, present, and future: Part 1. Crit. Rev. Biomed. Eng. 29 (5-6), 441–600. https://doi.org/10.1615/critrevbiomedeng.v29.i56.10.

Goldsmith, W., Monson, K.L., 2005. The state of head injury biomechanics: past, present, and future Part 2: physical experimentation. Crit. Rev. Biomed. Eng. 33 (2), 105–207. https://doi.org/10.1615/critrevbiomedeng.v33.i2.20.

Haber, M., Hutchinson, E.B., Sadeghi, N., Cheng, W.H., Namjoshi, D., Cripton, P., Irfanoglu, M.O., Wellington, C., Diaz-Arrastia, R., Pierpaoli, C., 2017. Defining an analytic framework to evaluate quantitative MRI markers of traumatic axonal injury: preliminary results in a mouse closed head injury model. eNeuro 4 (5). https://doi.org/10.1523/ENEURO.0164-17.2017.

Hajiaghamemar, M., Seidi, M., Oeur, R.A., Margulies, S.S., 2019. Toward development of clinically translatable diagnostic and prognostic metrics of traumatic brain injury using animal models: a review and a look forward. Exp. Neurol. 318, 101–123. https://doi.org/10.1016/j.expneurol.2019.04.019.

Hardy, W.N., Foster, C.D., Mason, M.J., Yang, K.H., King, A.I., Tashman, S., 2001. Investigation of head injury mechanisms using neutral density technology and high-speed biplanar X-ray. Stapp. Car Crash. J. 45, 337–368. http://www.stapp.org/pubs.shtml.

Harrison, J.L., Rowe, R.K., Ellis, T.W., Yee, N.S., O'Hara, B.F., Adelson, P.D., Lifshitz, J., 2015. Resolvins AT-D1 and E1 differentially impact functional outcome, post-traumatic sleep, and microglial activation following diffuse brain injury in the mouse. Brain Behav. Immun. 47, 131–140. https://doi.org/10.1016/j.bbi.2015.01.001.

Henry, J.M., Talukder, N.K., Lee Jr., A.B., Walker, M.L., 1997. Cerebral trauma-induced changes in corpus striatal dopamine receptor subtypes. J. Investig. Surg. 10 (5), 281–286. https://doi.org/10.3109/08941939709032167.

Hernandez, A., Donovan, V., Grinberg, Y.Y., Obenaus, A., Carson, M.J., 2016. Differential detection of impact site versus rotational site injury by magnetic resonance imaging and microglial morphology in an unrestrained mild closed head injury model. J. Neurochem. 136 (Suppl. 1), 18–28. https://doi.org/10.1111/jnc.13402.

Hicks, R., Giacino, J., Harrison-Felix, C., Manley, G., Valadka, A., Wilde, E.A., 2013.

Progress in developing common data elements for traumatic brain injury research: version two – the end of the beginning. J. Neurotrauma 30 (22), 1852–1861. https://doi.org/10.1089/neu.2013.2938.

Holbourn, A., 1943. Mechanics of head injuries. Lancet 242 (6267), 438–441. https://doi.org/10.1016/S0140-6736(00)87453-X.

Huang, E.Y., Tsui, P.-F., Kuo, T.T., Tsai, J.J., Chou, Y.C., Ma, H.I., Chiang, Y.H., Chen, Y.H., 2014. Amantadine ameliorates dopamine-releasing deficits and behavioral deficits in rats after fluid percussion injury. PLoS One 9 (1), e86354. https://doi.org/10.1371/journal.pone.0086354.

Hutchinson, E.B., Schwerin, S.C., Avram, A.V., Juliano, S.L., Pierpaoli, C., 2018. Diffusion MRI and the detection of alterations following traumatic brain injury. J. Neurosci. Res. 96 (4), 612–625. https://doi.org/10.1002/jnr.24065.

Illouz, T., Madar, R., Clague, C., Griffioen, K.J., Louzoun, Y., Okun, E., 2016. Unbiased classification of spatial strategies in the Barnes maze. Bioinformatics 32 (21), 3314–3320. https://doi.org/10.1093/bioinformatics/btw376. (Oxford, England).

James, S.L., Theadom, A., Ellenbogen, R.G., Bannick, M.S., Montjoy-Venning, W., Lucchesi, L.R., Abbasi, N., Abdulkader, R., Abraha, H.N., Adsuar, J.C., Afarideh, M., Agrawal, S., Ahmadi, A., Ahmed, M.B., Aichour, A.N., Aichour, I., Aichour, M.T.E., Akinyemi, R.O., Akseer, N., Alahdab, F., Alebel, A., Alghnam, S.A., Ali, B.A., Alsharif, U., Altirkawi, K., Andrei, C.L., Anjomshoa, M., Ansari, H., Ansha, M.G., Antonio, C.A.T., Appiah, S.C.Y., Ariani, F., Asefa, N.G., Asgedom, S.W., Atique, S., Awasthi, A., Ayala Quintanilla, B.P., Ayuk, T.B., Azzopardi, P.S., Badali, H., Badawi, A., Balalla, S., Banstola, A., Barker-Collo, S.L., Bärnighausen, T.W., Bedi, N., Behzadifar, M., Behzadifar, M., Bekele, B.B., Belachew, A.B., Belay, Y.A., Bennett, D.A., Bensenor, I.M., Berhane, A., Beuran, M., Bhalla, A., Bhaumik, S., Bhutta, Z.A., Biadgo, B., Biffino, M., Bijani, A., Bililign, N., Birungi, C., Boufous, S., Brazinova, A., Brown, A.W., Car, M., Cárdenas, R., Carrero, J.J., Carvalho, F., Castañeda-Orjuela, C.A., Catalá-López, F., Chaiah, Y., Champs, A.P., Chang, J.-C., Choi, J.-Y.J., Christopher, D.J., Cooper, C., Crowe, C.S., Dandona, L., Dandona, R., Daryani, A., Davitoiu, D.V., Degefa, M.G., Demoz, G.T., Deribe, K., Djalalinia, S., Do, H.P., Doku, D.T., Drake, T.M., Dubey, M., Dubljanin, E., El-Khatib, Z., Ofori-Asenso, R., Eskandarieh, S., Esteghamati, A., Esteghamati, S., Faro, A., Farzadfar, F., Farzaei, M.H., Fereshtehnejad, S.-M., Fernandes, E., Feyissa, G.T., Filip, I., Fischer, F., Fukumoto, T., Ganji, M., Gankpe, F.G., Gebre, A.K., Gebrehiwot, T.T., Gezae, K.E., Gopalkrishna, G., Goulart, A.C., Haagsma, J.A., Haj-Mirzaian, A., Haj-Mirzaian, A., Hamadeh, R.R., Hamidi, S., Haro, J.M., Hassankhani, H., Hassen, H.Y., Havmoeller, R., Hawley, C., Hay, S.I., Hegazy, M.I., Hendrie, D., Henok, A., Hibstu, D.T., Hoffman, H.J., Hole, M.K., Homaie Rad, E., Hosseini, S.M., Hostiuc, S., Hu, G., Hussen, M.A., Ilesanmi, O.S., Irvani, S.S.N., Jakovljevic, M., Jayaraman, S., Jha, R.P., Jonas, J.B., Jones, K.M., Jorjoran Shushtari, Z., Jozwiak, J.J., Jürisson, M., Kabir, A., Kahsay, A., Kahssay, M., Kalani, R., Karch, A., Kasaeian, A., Kassa, G.M., Kassa, T.D., Kassa, Z.Y., Kengne, A.P., Khader, Y.S., Khafaie, M.A., Khalid, N., Khalil, I., Khan, E.A., Khan, M.S., Khang, Y.-H., Khazaie, H., Khoja, A.T., Khubchandani, J., Kiadaliri, A.A., Kim, D., Kim, Y.-E., Kisa, A., Koyanagi, A., Krohn, K.J., Kuate Defo, B., Kucuk Bicer, B., Kumar, G.A., Kumar, M., Lalloo, R., Lami, F.H., Lansingh, V.C., Laryea, D.O., Latifi, A., Leshargie, C.T., Levi, M., Li, S., Liben, M.L., Lotufo, P.A., Lunevicius, R., Mahotra, N.B., Majdan, M., Majeed, A., Malekzadeh, R., Manda, A.-L., Mansournia, M.A., Massenburg, B.B., Mate, K.K.V., Mehndiratta, M.M., Mehta, V., Meles, H., Melese, A., Memiah, P.T.N., Mendoza, W., Mengistu, G., Meretoja, A., Meretoja, T.J., Mestrovic, T., Miazgowski, T., Miller, T.R., Mini, G.K., Mirica, A., Mirrakhimov, E.M., Moazen, B., Mohammadi, M., Molokhia, M., Monasta, L., Mondello, S., Moosazadeh, M., Moradi, G., Moradi, M., Moradi-Lakeh, M., Moradinazar, M., Morrison, S.D., Moschos, M.M., Mousavi, S.M., Murthy, S., Musa, K.I., Mustafa, G., Naghavi, M., Naik, G., Najafi, F., Nangia, V., Nascimento, B.R., Negoi, I., Nguyen, T.H., Nichols, E., Ningrum, D.N.A., Nirayo, Y.L., Nyasulu, P.S., Ogbo, F.A., Oh, I.-H., Okoro, A., Olagunju, A.T., Olagunju, T.O., Olivares, P.R., Otstavnov, S.S., Owolabi, M.O., P A, M., Pakhale, S., Pandey, A.R., Pesudovs, K., Pinilla-Monsalve, G.D., Polinder, S., Poustchi, H., Prakash, S., Qorbani, M., Radfar, A., Rafay, A., Rafiei, A., Rahimi-Movaghar, A., Rahimi-Movaghar, V., Rahman, M., Rahman, M.A., Rai, R.K., Rajati, F., Ram, U., Rawaf, D.L., Rawaf, S., Reiner, R.C., Reis, C., Renzaho, A.M.N., Resnikoff, S., Rezaei, S., Rezaeian, S., Roever, L., Ronfani, L., Roshandel, G., Roy, N., Ruhago, G.M., Saddik, B., Safari, H., Safiri, S., Sahraian, M.A., Salamati, P., Saldanha, R.d.F., Samy, A.M., Sanabria, J., Santos, J.V., Santric Milicevic, M.M.M., Sartorius, B., Satpathy, M., Savuon, K., Schneider, I.J.C., Schwebel, D.C., Sepanlou, S.G., Shabaninejad, H., Shaikh, M.A.A., Shams-Beyranvand, M., Sharif, M., Sharif-Alhoseini, M., Shariful Islam, S.M., She, J., Sheikh, A., Shen, J., Sheth, K.N., Shibuya, K., Shiferaw, M.S., Shigematsu, M., Shiri, R., Shiue, I., Shoman, H., Siabani, S., Siddiqi, T.J., Silva, J.P., Silveira, D.G.A., Sinha, D.N., Smith, M., Soares Filho, A.M., Sobhani, S., Soofi, M., Soriano, J.B., Soyiri, I.N., Stein, D.J., Stokes, M.A., Sufiyan, M.a.B., Sunguya, B.F., Sunshine, J.E., Sykes, B.L., Szoeke, C.E.I., Tabarés-Seisdedos, R., Te Ao, B.J., Tehrani-Banihashemi, A., Tekle, M.G., Temsah, M.-H., Temsah, O., Topor-Madry, R., Tortajada-Girbés, M., Tran, B.X., Tran, K.B., Tudor Car, L., Ukwaja, K.N., Ullah, I., Usman, M.S., Uthman, O.A., Valdez, P.R., Vasankari, T.J., Venketasubramanian, N., Violante, F.S., Wagnew, F.W.S., Waheed, Y., Wang, Y.-P., Weldegwergs, K.G., Werdecker, A., Wijeratne, T., Winkler, A.S., Wyper, G.M.A., Yano, Y., Yaseri, M., Yasin, Y.J., Ye, P., Yimer, E.M., Yip, P., Yisma, E., Yonemoto, N., Yoon, S.-J., Yost, M.G., Younis, M.Z., Yousefifard, M., Yu, C., Zaidi, Z., Zaman, S.B., Zamani, M., Zenebe, Z.M., Zodpey, S., Feigin, V.L., Vos, T., Murray, C.J.L., 2019. Global, regional, and national burden of traumatic brain injury and spinal cord injury, 1990–2016: a systematic analysis for the Global Burden of Disease Study 2016. Lancet Neurol. 18 (1), 56–87. https://doi.org/10.1016/s1474-4422(18)30415-0.

Jamnia, N., Urban, J.H., Stutzmann, G.E., Chiren, S.G., Reisenbigler, E., Marr, R., Peterson, D., Kozlowski, D.A., 2017. A clinically relevant closed-head model of single and repeat concussive injury in the adult rat using a controlled cortical impact device. J. Neurotrauma 34 (7), 1351–1363. https://doi.org/10.1089/neu.2016.4517.

Johnson, V.E., Stewart, W., Smith, D.H., 2012. Widespread tau and amyloid-beta

pathology many years after a single traumatic brain injury in humans. Brain Pathol. 22 (2), 142–149. https://doi.org/10.1111/j.1750-3639.2011.00513.x.

Johnson, V.E., Stewart, J.E., Begbie, F.D., Trojanowski, J.Q., Smith, D.H., Stewart, W., 2013. Inflammation and white matter degeneration persist for years after a single traumatic brain injury. Brain 136 (Pt 1), 28–42. https://doi.org/10.1093/brain/aws322.

Kane, M.J., Angoa-Pérez, M., Briggs, D.I., Viano, D.C., Kreipke, C.W., Kuhn, D.M., 2012. A mouse model of human repetitive mild traumatic brain injury. J. Neurosci. Methods 203 (1), 41–49. https://doi.org/10.1016/j.jneumeth.2011.09.003.

Kikinis, Z., Muehlmann, M., Pasternak, O., Peled, S., Kulkarni, P., Ferris, C., Bouix, S., Rathi, Y., Koerte, I.K., Pieper, S., Yarmarkovich, A., Porter, C.L., Kristal, B.S., Shenton, M.E., 2017. Diffusion imaging of mild traumatic brain injury in the impact accelerated rodent model: a pilot study. Brain Inj. 31 (10), 1376–1381. https://doi.org/10.1080/02699052.2017.1318450.

Kilbourne, M., Kuehn, R., Tosun, C., Caridi, J., Keledjian, K., Bochicchio, G., Scalea, T., Gerzanich, V., Simard, J.M., 2009. Novel model of frontal impact closed head injury in the rat. J. Neurotrauma 26 (12), 2233–2243. https://doi.org/10.1089/neu.2009.0968.

Klemenhagen, K.C., O'Brien, S.P., Brody, D.L., 2013. Repetitive concussive traumatic brain injury interacts with post-injury foot shock stress to worsen social and depression-like behavior in mice. PLoS One 8 (9), e74510. https://doi.org/10.1371/journal.pone.0074510.

Komlosh, M.E., Benjamini, D., Hutchinson, E.B., King, S., Haber, M., Avram, A.V., Holtzclaw, L.A., Desai, A., Pierpaoli, C., Basser, P.J., 2018. Using double pulsed-field gradient MRI to study tissue microstructure in traumatic brain injury (TBI). Microporous Mesoporous Mater. 269, 156–159. https://doi.org/10.1016/j.micromeso.2017.05.030.

Krukowski, K., Nolan, A., Frias, E., Grue, K., Becker, M., Ureta, G., Delgado, L., Bernales, S., Sohal, V.S., Walter, P., Rosi, S., 2020. Integrated stress response inhibitor reverses sex-dependent behavioral and cell-specific deficits after mild repetitive head trauma. J. Neurotrauma. https://doi.org/10.1089/neu.2019.6827.

Kupferberg, A., Bicks, L., Hasler, G., 2016. Social functioning in major depressive disorder. Neurosci. Biobehav. Rev. 69, 313–332. https://doi.org/10.1016/j.neubiorev.2016.07.002.

LaPlaca, M.C., Simon, C.M., Prado, G.R., Cullen, D.K., 2007. CNS injury biomechanics and experimental models. Prog. Brain Res. 161, 13–26. https://doi.org/10.1016/S0079-6123(06)61002-9.

Leary, J.B., Bondi, C.O., LaPorte, M.J., Carlson, L.J., Radabaugh, H.L., Cheng, J.P., Kline, A.E., 2017. The therapeutic efficacy of environmental enrichment and methylphenidate alone and in combination after controlled cortical impact injury. J. Neurotrauma 34 (2), 444–450. https://doi.org/10.1089/neu.2016.4438.

Li, H., Zhang, C., Yang, C., Blevins, M., Norris, D., Zhao, R., Huang, M., 2020. C-terminal binding proteins 1 and 2 in traumatic brain injury-induced inflammation and their inhibition as an approach for anti-inflammatory treatment. Int. J. Biol. Sci. 16 (7), 1107–1120. https://doi.org/10.7150/ijbs.42109.

Lighthall, J.W., 1988. Controlled cortical impact: a new experimental brain injury model. J. Neurotrauma 5 (1), 1–15. https://doi.org/10.1089/neu.1988.5.1.

Lighthall, J.W., Dixon, C.E., Anderson, T.E., 1989. Experimental models of brain injury. J. Neurotrauma 6 (2), 83–97. https://doi.org/10.1089/neu.1989.6.83.

Lister, R.G., 1987. The use of a plus-maze to measure anxiety in the mouse. Psychopharmacology 92 (2), 180–185. https://doi.org/10.1007/BF00177912.

Liu, X., Qiu, J., Alcon, S., Hashim, J., Meehan 3rd, W.P., Mannix, R., 2017. Environmental enrichment mitigates deficits after repetitive mild traumatic brain injury. J. Neurotrauma 34 (16), 2445–2455. https://doi.org/10.1089/neu.2016.4823.

Mac Donald, C.L., Dikranian, K., Song, S.K., Bayly, P.V., Holtzman, D.M., Brody, D.L., 2007. Detection of traumatic axonal injury with diffusion tensor imaging in a mouse model of traumatic brain injury. Exp. Neurol. 205 (1), 116–131. https://doi.org/10.1016/j.expneurol.2007.01.035.

Mahar, I., Alosco, M.L., McKee, A.C., 2017. Psychiatric phenotypes in chronic traumatic encephalopathy. Neurosci. Biobehav. Rev. 83, 622–630. https://doi.org/10.1016/j.neubiorev.2017.08.023.

Malkesman, O., Tucker, L.B., Ozl, J., McCabe, J.T., 2013. Traumatic brain injury - modeling neuropsychiatric symptoms in rodents. Front. Neurol. 4, 157. https://doi.org/10.3389/fneur.2013.00157.

Mannix, R., Berglass, J., Berkner, J., Moleus, P., Qiu, J., Andrews, N., Gunner, G., Berglass, L., Jantzie, L.L., Robinson, S., Meehan 3rd, W.P., 2014. Chronic gliosis and behavioral deficits in mice following repetitive mild traumatic brain injury. J. Neurosurg. 121 (6), 1342–1350. https://doi.org/10.3171/2014.7.jns14272.

Margulies, S.S., Thibault, L.E., 1992. A proposed tolerance criterion for diffuse axonal injury in man. J. Biomech. 25 (8), 917–923. https://doi.org/10.1016/0021-9290(92)90231-0.

Margulies, S.S., Thibault, L.E., Gennarelli, T.A., 1990. Physical model simulations of brain injury in the primate. J. Biomech. 23 (8), 823–836. https://doi.org/10.1016/0021-9290(90)90029-3.

Marmarou, A., Foda, M.A., van den Brink, W., Campbell, J., Kita, H., Demetriadou, K., 1994. A new model of diffuse brain injury in rats. Part I: Pathophysiology and biomechanics. J. Neurosurg. 80 (2), 291–300. https://doi.org/10.3171/jns.1994.80.2.0291.

Maxwell, W.L., Watt, C., Graham, D.I., Gennarelli, T.A., 1993. Ultrastructural evidence of axonal shearing as a result of lateral acceleration of the head in non-human primates. Acta Neuropathol. Commun. 86 (2), 136–144. https://doi.org/10.1007/bf00334880.

McInnes, K.A., Abebe, Z., Whyte, T., Bashir, A., Barron, C., Wellington, C., Cripton, P.A., 2020. An automated kinematic measurement system for sagittal plane murine head impacts. J. Biomech. Eng. https://doi.org/10.1115/1.4046202. 10.1115/1.4046202.

McIntosh, T.K., Smith, D.H., Voddi, M., Perri, B.R., Stutzmann, J.M., 1996. Riluzole, a

novel neuroprotective agent, attenuates both neurologic motor and cognitive dysfunction following experimental brain injury in the rat. J. Neurotrauma 13 (12), 767–780. https://doi.org/10.1089/neu.1996.13.767.

McKee, A.C., Cantu, R.C., Nowinski, C.J., Hedley-Whyte, E.T., Gavett, B.E., Budson, A.E., Santini, V.E., Lee, H.S., Kubilus, C.A., Stern, R.A., 2009. Chronic traumatic encephalopathy in athletes: progressive tauopathy after repetitive head injury. J. Neuropathol. Exp. Neurol. 68 (7), 709–735. https://doi.org/10.1097/NEN.0b013e3181a9d503.

Meaney, D.F., Smith, D.H., Shreiber, D.I., Bain, A.C., Miller, R.T., Ross, D.T., Gennarelli, T.A., 1995. Biomechanical analysis of experimental diffuse axonal injury. J. Neurotrauma 12 (4), 689–694. https://doi.org/10.1089/neu.1995.12.689.

Mouzon, B.C., Bachmeier, C., Ferro, A., Ojo, J.O., Crynen, G., Acker, C.M., Davies, P., Mullan, M., Stewart, W., Crawford, F., 2014. Chronic neuropathological and neurobehavioral changes in a repetitive mild traumatic brain injury model. Ann. Neurol. 75 (2), 241–254. https://doi.org/10.1002/ana.24064.

Moy, S.S., Nadler, J.J., Perez, A., Barbaro, R.P., Johns, J.M., Magnuson, T.R., Piven, J., Crawley, J.N., 2004. Sociability and preference for social novelty in five inbred strains: an approach to assess autistic-like behavior in mice. Genes Brain Behav. 3 (5), 287–302. https://doi.org/10.1111/j.1601-1848.2004.00076.x.

Mychasiuk, R., Hehar, H., Candy, S., Ma, I., Esser, M.J., 2016. The direction of the acceleration and rotational forces associated with mild traumatic brain injury in rodents effect behavioural and molecular outcomes. J. Neurosci. Methods 257, 168–178. https://doi.org/10.1016/j.jneumeth.2015.10.002.

Namjoshi, D.R., Cheng, W.H., McInnes, K.A., Martens, K.M., Carr, M., Wilkinson, A., Fan, J., Robert, J., Hayat, A., Cripton, P.A., Wellington, C.L., 2014. Merging pathology with biomechanics using CHIMERA (Closed-Head Impact Model of Engineered Rotational Acceleration): a novel, surgery-free model of traumatic brain injury. Mol. Neurodegener. 9, 55. https://doi.org/10.1186/1750-1326-9-55.

Namjoshi, D.R., Cheng, W.H., Carr, M., Martens, K.M., Zareyan, S., Wilkinson, A., McInnes, K.A., Cripton, P.A., Wellington, C.L., 2016. Chronic exposure to androgenic-anabolic steroids exacerbates axonal injury and microgliosis in the CHIMERA mouse model of repetitive concussion. PLoS One 11 (1), e0146540. https://doi.org/10.1371/journal.pone.0146540.

Namjoshi, D.R., Cheng, W.H., Bashir, A., Wilkinson, A., Stukas, S., Martens, K.M., Whyte, T., Abebe, Z.A., McInnes, K.A., Cripton, P.A., Wellington, C.L., 2017. Defining the biomechanical and biological threshold of murine mild traumatic brain injury using CHIMERA (Closed Head Impact Model of Engineered Rotational Acceleration). Exp. Neurol. 292, 80–91. https://doi.org/10.1016/j.expneurol.2017.03.003.

National Research Council Committee on Sports-Related Concussions in Youth, 2014. Sports-Related Concussions in Youth: Improving the Science, Changing the Culture. National Academies Press, Washington, DC.

Nolan, A., Hennessy, E., Krukowski, K., Guglielmetti, C., Chaumeil, M.M., Sohal, V.S., Rosi, S., 2018. Repeated mild head injury leads to wide-ranging deficits in higher-order cognitive functions associated with the prefrontal cortex. J. Neurotrauma 35 (20), 2425–2434. https://doi.org/10.1089/neu.2018.5731.

Ommaya, A.K., Hirsch, A.E., Flamm, E.S., Mahone, R.H., 1966. Cerebral concussion in the monkey: an experimental model. Science 153 (3732), 211–212.

Osier, N.D., Carlson, S.W., DeSana, A., Dixon, C.E., 2015. Chronic histopathological and behavioral outcomes of experimental traumatic brain injury in adult male animals. J. Neurotrauma 32 (23), 1861–1882. https://doi.org/10.1089/neu.2014.3680.

Pautler, R.G., 2004. Mouse MRI: concepts and applications in physiology. Physiology 19 (4), 168–175. https://doi.org/10.1152/physiol.00016.2004. (Bethesda).

Petraglia, A.L., Plog, B.A., Dayawansa, S., Chen, M., Dashnaw, M.L., Czerniecka, K., Walker, C.T., Viterise, T., Hyrien, O., Iliff, J.J., Deane, R., Nedergaard, M., Huang, J.H., 2014. The spectrum of neurobehavioral sequelae after repetitive mild traumatic brain injury: a novel mouse model of chronic traumatic encephalopathy. J. Neurotrauma 31 (13), 1211–1224. https://doi.org/10.1089/neu.2013.3255.

Popovitz, J., Mysore, S.P., Adwanikar, H., 2019. Long-term effects of traumatic brain injury on anxiety-like behaviors in mice: behavioral and neural correlates. Front. Behav. Neurosci. 13, 6. https://doi.org/10.3389/fnbeh.2019.00006.

Prins, M.L., Hales, A., Reger, M., Giza, C.C., Hovda, D.A., 2010. Repeat traumatic brain injury in the juvenile rat is associated with increased axonal injury and cognitive impairments. Dev. Neurosci. 32 (5-6), 510–518. https://doi.org/10.1159/000316800.

Rowson, S., Duma, S.M., Beckwith, J.G., Chu, J.J., Greenwald, R.M., Crisco, J.J., Brolinson, P.G., Duhaime, A.C., McAllister, T.W., Maerlender, A.C., 2012. Rotational head kinematics in football impacts: an injury risk function for concussion. Ann. Biomed. Eng. 40 (1), 1–13. https://doi.org/10.1007/s10439-011-0392-4.

Saatman, K.E., Murai, H., Bartus, R.T., Smith, D.H., Hayward, N.J., Perri, B.R., McIntosh, T.K., 1996. Calpain inhibitor AK295 attenuates motor and cognitive deficits following experimental brain injury in the rat. Proc. Natl. Acad. Sci. U. S. A. 93 (8), 3428–3433. https://doi.org/10.1073/pnas.93.8.3428.

Sauerbeck, A.D., Fanizzi, C., Kim, J.H., Gangolli, M., Bayly, P.V., Wellington, C.L., Brody, D.L., Kummer, T.T., 2018. modCHIMERA: a novel murine closed-head model of moderate traumatic brain injury. Sci. Rep. 8 (1), 7677. https://doi.org/10.1038/s41598-018-25737-6.

Sauerbeck, A.D., Gangolli, M., Reitz, S.J., Salyards, M.H., Kim, S.H., Hemingway, C., Gratuze, M., Makkapati, T., Kerschensteiner, M., Holtzman, D.M., Brody, D.L., Kummer, T.T., 2020. SEQUIN multiscale imaging of mammalian central synapses reveals loss of synaptic connectivity resulting from diffuse traumatic brain injury. Neuron, in press. https://doi.org/10.1016/j.neuron.2020.04.012.

Sawyer, T.W., Wang, Y., Ritzel, D.V., Josey, T., Villanueva, M., Shei, Y., Nelson, P., Hennes, G., Weiss, T., Vair, C., Fan, C., Barnes, J., 2016. High-fidelity simulation of primary blast: direct effects on the head. J. Neurotrauma 33 (13), 1181–1193. https://doi.org/10.1089/neu.2015.3914.

Schmitt, S., Dichter, M.A., 2015. Electrophysiologic recordings in traumatic brain injury.

Handb. Clin. Neurol. 127, 319–339. https://doi.org/10.1016/B978-0-444-52892-6.00021-0.

Skotak, M., Townsend, M.T., Ramarao, K.V., Chandra, N., 2019. A comprehensive review of experimental rodent models of repeated blast TBI. Front. Neurol. 10, 1015. https://doi.org/10.3389/fneur.2019.01015.

Smith, D.H., Soares, H.D., Pierce, J.S., Perlman, K.G., Saatman, K.E., Meaney, D.F., Dixon, C.E., McIntosh, T.K., 1995. A model of parasagittal controlled cortical impact in the mouse: cognitive and histopathologic effects. J. Neurotrauma 12 (2), 169–178. https://doi.org/10.1089/neu.1995.12.169.

Smith, D.H., Hicks, R.R., Johnson, V.E., Bergstrom, D.A., Cummings, D.M., Noble, L.J., Hovda, D., Whalen, M., Ahlers, S.T., LaPlaca, M., Tortella, F.C., Duhaime, A.C., Dixon, C.E., 2015. Pre-clinical traumatic brain injury common data elements: toward a common language across laboratories. J. Neurotrauma 32 (22), 1725–1735. https://doi.org/10.1089/neu.2014.3861.

Stemper, B.D., Shah, A.S., Pintar, F.A., McCrea, M., Kurpad, S.N., Glavaski-Joksimovic, A., Olsen, C., Budde, M.D., 2015. Head rotational acceleration characteristics influence behavioral and diffusion tensor imaging outcomes following concussion. Ann. Biomed. Eng. 43 (5), 1071–1088. https://doi.org/10.1007/s10439-014-1171-9.

Steru, L., Chermat, R., Thierry, B., Simon, P., 1985. The tail suspension test: a new method for screening antidepressants in mice. Psychopharmacology 85 (3), 367–370. https://doi.org/10.1007/bf00428203.

Sullivan, S., Eucker, S.A., Gabrieli, D., Bradfield, C., Coats, B., Maltese, M.R., Lee, J., Smith, C., Margulies, S.S., 2015. White matter tract-oriented deformation predicts traumatic axonal brain injury and reveals rotational direction-specific vulnerabilities. Biomech. Model. Mechanobiol. 14 (4), 877–896. https://doi.org/10.1007/s10237-014-0643-z.

Tchantchou, F., Tucker, L.B., Fu, A.H., Bluett, R.J., McCabe, J.T., Patel, S., Zhang, Y., 2014. The fatty acid amide hydrolase inhibitor PF-3845 promotes neuronal survival, attenuates inflammation and improves functional recovery in mice with traumatic brain injury. Neuropharmacology 85C, 427–439. https://doi.org/10.1016/j.neuropharm.2014.06.006.

Te Ao, B., Brown, P., Tobias, M., Ameratunga, S., Barker-Collo, S., Theadom, A., McPherson, K., Starkey, N., Dowell, A., Jones, K., Feigin, V.L., Group, B.S., 2014. Cost of traumatic brain injury in New Zealand: evidence from a population-based study. Neurology 83 (18), 1645–1652. https://doi.org/10.1212/WNL.0000000000000933.

Thurmond, V.A., Hicks, R., Gleason, T., Miller, A.C., Szuflita, N., Orman, J., Schwab, K., 2010. Advancing integrated research in psychological health and traumatic brain injury: common data elements. Arch. Phys. Med. Rehabil. 91 (11), 1633–1636. https://doi.org/10.1016/j.apmr.2010.06.034.

Tucker, L.B., Fu, A.H., McCabe, J.T., 2016. Performance of male and female C57BL/6J mice on motor and cognitive tasks commonly used in pre-clinical traumatic brain injury research. J. Neurotrauma 33 (9), 880–894. https://doi.org/10.1089/neu.2015.3977.

Tucker, L.B., Burke, J.F., Fu, A.H., McCabe, J.T., 2017. Neuropsychiatric symptom modeling in male and female C57BL/6J mice after experimental traumatic brain injury. J. Neurotrauma 34 (4), 890–905. https://doi.org/10.1089/neu.2016.4508.

Tucker, L.B., Velosky, A.G., McCabe, J.T., 2018. Applications of the Morris water maze in translational traumatic brain injury research. Neurosci. Biobehav. Rev. 88, 187–200. https://doi.org/10.1016/j.neubiorev.2018.03.010.

Tucker, L.B., Velosky, A.G., Fu, A.H., McCabe, J.T., 2019. Chronic neurobehavioral sex differences in a murine model of repetitive concussive brain injury. Front. Neurol. 10, 509. https://doi.org/10.3389/fneur.2019.00509.

U.S. Department of Defense, 2019. Traumatic Brain Injury Website. Date Accessed May 21, 2019. (http://dod.defense.gov/News/Special-Reports/0315_tbi/).

University of British Columbia Wellington Laboratory and the Orthopedics and Injury Biomechanics Group, 2017. CHIMERA Reference Manual, Version 2.0, December, 2017. p. 32.

Velosky, A.G., Tucker, L.B., Fu, A.H., Liu, J., McCabe, J.T., 2017. Cognitive performance of male and female C57BL/6J mice after repetitive concussive brain injuries. Behav. Brain Res. 324, 115–124. https://doi.org/10.1016/j.bbr.2017.02.017.

Viano, D.C., Hamberger, A., Bolouri, H., Säljö, A., 2009. Concussion in professional football: animal model of brain injury – part 15. Neurosurgery 64 (6), 1162–1173. https://doi.org/10.1227/01.NEU.0000345863.99099.C7.

Vonder Haar, C., Martens, K.M., Bashir, A., McInnes, K.A., Cheng, W.H., Cheung, H., Stukas, S., Barron, C., Ladner, T., Welch, K.A., Cripton, P.A., Winstanley, C.A., Wellington, C.L., 2019. Repetitive closed-head impact model of engineered rotational acceleration (CHIMERA) injury in rats increases impulsivity, decreases dopaminergic innervation in the olfactory tubercle and generates white matter inflammation, tau phosphorylation and degeneration. Exp. Neurol. 317, 87–99. https://doi.org/10.1016/j.expneurol.2019.02.012.

Wagner, A.K., Kline, A.E., Ren, D., Willard, L.A., Wenger, M.K., Zafonte, R.D., Dixon, C.E., 2007. Gender associations with chronic methylphenidate treatment and behavioral performance following experimental traumatic brain injury. Behav. Brain Res. 181 (2), 200–209. https://doi.org/10.1016/j.bbr.2007.04.006.

Wakade, C., Sukumari-Ramesh, S., Laird, M.D., Dhandapani, K.M., Vender, J.R., 2010. Delayed reduction in hippocampal postsynaptic density protein-95 expression temporally correlates with cognitive dysfunction following controlled cortical impact in mice. J. Neurosurg. 113 (6), 1195–1201. https://doi.org/10.3171/2010.3.JNS091212.

Washington, P.M., Forcelli, P.A., Wilkins, T., Zapple, D.N., Parsadanian, M., Burns, M.P., 2012. The effect of injury severity on behavior: a phenotypic study of cognitive and emotional deficits after mild, moderate, and severe controlled cortical impact injury in mice. J. Neurotrauma 29 (13), 2283–2296. https://doi.org/10.1089/neu.2012.2456.

Watanabe, J., Shetty, A.K., Hattiangady, B., Kim, D.-K., Foraker, J.E., Nishida, H., Prockop, D.J., 2013. Administration of TSG-6 improves memory after traumatic brain

injury in mice. Neurobiol. Dis. 59 (0), 86–99. https://doi.org/10.1016/j.nbd.2013. 06.017.

Weber, M.T., Arena, J.D., Xiao, R., Wolf, J.A., Johnson, V.E., 2019. CLARITY reveals a more protracted temporal course of axon swelling and disconnection than previously described following traumatic brain injury. Brain Pathol. 29 (3), 437–450. https:// doi.org/10.1111/bpa.12677.

Whyte, T., Liu, J., Chung, V., McErlane, S.A., Abebe, Z.A., McInnes, K.A., Wellington, C.L., Cripton, P.A., 2019. Technique and preliminary findings for *in vivo* quantification of brain motion during injurious head impacts. J. Biomech. 95, 109279. https://doi. org/10.1016/j.jbiomech.2019.07.023.

Wojnarowicz, M.W., Fisher, A.M., Minaeva, O., Goldstein, L.E., 2017. Considerations for experimental animal models of concussion, traumatic brain injury, and chronic traumatic encephalopathy-these matters matter. Front. Neurol. 8, 240. https://doi. org/10.3389/fneur.2017.00240.

Yang, Z., Wang, P., Morgan, D., Lin, D., Pan, J., Lin, F., Strang, K.H., Selig, T.M., Perez, P.D., Febo, M., Chang, B., Rubenstein, R., Wang, K.K., 2015. Temporal MRI characterization, neurobiochemical and neurobehavioral changes in a mouse repetitive concussive head injury model. Sci. Rep. 5, 11178. https://doi.org/10.1038/ srep11178.

Yin, T.C., Voorhees, J.R., Genova, R.M., Davis, K.C., Madison, A.M., Britt, J.K., Cintrón-Pérez, C.J., McDaniel, L., Harper, M.M., Pieper, A.A., 2016. Acute axonal degeneration drives development of cognitive, motor, and visual deficits after blast-mediated traumatic brain injury in mice. eNeuro 3 (5). https://doi.org/10.1523/ENEURO. 0220-16.2016.

Yu, F., Wang, Z., Tchantchou, F., Chiu, C.T., Zhang, Y., Chuang, D.M., 2012. Lithium ameliorates neurodegeneration, suppresses neuroinflammation, and improves behavioral performance in a mouse model of traumatic brain injury. J. Neurotrauma 29 (2), 362–374. https://doi.org/10.1089/neu.2011.1942.

Yu, F., Shukla, D.K., Armstrong, R.C., Marion, C.M., Radomski, K.L., Selwyn, R.G., Dardzinski, B.J., 2017. Repetitive model of mild traumatic brain injury produces cortical abnormalities detectable by magnetic resonance diffusion imaging, histopathology, and behavior. J. Neurotrauma 34 (7), 1364–1381. https://doi.org/10. 1089/neu.2016.4569.

Zhang, A.L., Sing, D.C., Rugg, C.M., Feeley, B.T., Senter, C., 2016. The rise of concussions in the adolescent population. Orthop. J. Sports Med. 4 (8). https://doi.org/10.1177/ 2325967116662458. 2325967116662458.